Published in final edited form as:
J Comp Neurol. 2009 April 20; 513(6): 566–596. doi:10.1002/cne.21891.

The mesopontine rostromedial tegmental nucleus: a structure targeted by the lateral habenula that projects to the ventral tegmental area of Tsai and substantia nigra compacta

Thomas C. Jhou[1,*,#], **Stefanie Geisler**[2,#], **Michela Marinelli**[3], **Beth A. DeGarmo**[2], and **Daniel S. Zahm**[2,*]

[1]Department of Psychological and Brain Sciences, Johns Hopkins University, Ames Hall, 3400 Charles St., Baltimore, MD 21218

[2]Department of Pharmacological and Physiological Science, Saint Louis University School of Medicine, 1402 S. Grand Blvd., Saint Louis, MO 63104

[3]Dept. Cellular & Molecular Pharmacology, Rosalind Franklin University of Medicine and Science/ Chicago Medical School, 3333 Green Bay Rd, North Chicago, IL 60064

Abstract

Prior studies revealed that aversive stimuli and psychostimulant drugs elicit Fos expression in neurons clustered above and behind the interpeduncular nucleus that project strongly to the ventral tegmental area (VTA) and substantia nigra (SN) compacta (C). Other reports suggest that these neurons modulate responding to aversive stimuli. We now designate the region containing them as the mesopontine rostromedial tegmental nucleus (RMTg) and report herein on its neuroanatomy. Dense mu opioid receptor and somatostatin immunoreactivity characterize the RMTg, as do neurons projecting to the VTA/SNC that are enriched in GAD 67 mRNA. Strong inputs to the RMTg arise in the lateral habenula (LHb) and, to a lesser extent, the SN. Other inputs come from the frontal cortex, ventral striatopallidum, extended amygdala, septum, preoptic region, lateral, paraventricular and posterior hypothalamus, zona incerta, periaqueductal gray, intermediate layers of the contralateral superior colliculus, dorsal raphe, mesencephalic, pontine and medullary reticular formation, and the following nuclei: parafascicular, supramammillary, mammillary, ventral lateral geniculate, deep mesencephalic, red, pedunculopontine and laterodorsal tegmental, cuneiform, parabrachial and deep cerebellar. The RMTg has meager outputs to the forebrain, mainly to the ventral pallidum, preoptic-lateral hypothalamic continuum and midline-intralaminar thalamus, but much heavier outputs to the brainstem, including, most prominently, the VTA/SNC, as noted above, and to medial tegmentum, pedunculopontine and laterodorsal tegmental nuclei, dorsal raphe and the locus ceruleus and subceruleus. The RMTg may integrate multiple forebrain and brainstem inputs in relation to a dominant LHb input. Its outputs to neuromodulatory projection systems likely converge with direct LHb projections to those structures.

Keywords

midbrain tegmentum; reticular formation; dopaminergic regulation; locomotion

In considering the variety of brain structures activated following administration of the arousing drug, modafinil, Scammell et al. (2000) illustrated a conspicuous cluster of Fos-

[*]Corresponding authors: zahmds@slu.edu, (314) 977-8003, (314) 977-6411 [fax]. [*]tjhou@jhu.edu, (510) 316-0822.
[#]Present address: Behavioral Neuroscience Branch, National Institute on Drug Abuse, Biomedical Research Center, 251 Bayview Blvd, Baltimore, MD 21224

immunoreactive neurons, located suprajacent to the dorsolateral aspect of the caudal half of the interpeduncular nucleus, in a position they designated as "retroVTA." Chou et al. (2004) subsequently reported in an abstract that this region modulates conditioned and unconditioned freezing in response to fear-arousing stimuli and contains neurons that project to the ventral tegmental area (VTA) and substantia nigra (SN) compacta (C), of which a proportion is labeled with a probe against glutamate decarboxylase (GAD) 67 mRNA (see also Jhou, 20051). Perrotti et al. (2005), probably studying the same structure, but calling it the "posterior tail of the VTA", identified neurons in which ΔFosB, a long-lived splice variant of FosB (Hope et al., 1994), is expressed following chronic forced administration of psychostimulant drugs. Olson and Nestler (2007) demonstrated GAD immunoreactivity in neurons comprising a"ball-like" nucleus occupying the posteromedial VTA and speculated that it corresponds to the one described by Perrotti et al. (2005). Jhou and Gallagher (2007) reported in another abstract that VTA/SNC-projecting neurons in the region express Fos, the protein product of the immediate early gene, *c-fos* (Curran and Morgan, 1985; Morgan and Curran, 1986; Morgan et al., 1987; Sharp et al., 1993; Farvivar et al., 2004), in response to auditory cues associated with footshock, and that the region receives input from the lateral habenula (LHb). What is likely the same structure was discussed in a recent study of Fos-immunoreactive neurons observed following i.p. administration of D-amphetamine (Colussi-Mas et al., 2007), and these undoubtedly correspond to a cluster of neurons in the medial mesopontine tegmentum that projects to the VTA and prominently expresses Fos following administration of cocaine (Geisler et al., 2007b). The present study was undertaken to address cytoarchitecture, immunohistochemical markers and afferent and efferent connectivity that characterize this interesting brain structure, which, despite its lack of sharply delineated boundaries (Geisler et al., 2007b) and indeterminate neuronal composition, we will refer to as the rostromedial tegmental nucleus (RMTg), consistent with nomenclature attached to some other less than well-delimited mesopontine structures, such as the pedunculopontine (PPTg) and laterodorsal (LDTg) tegmental nuclei (Rye et al., 1987; Cornwall et al., 1990; Inglis and Winn, 1995).

Materials and Methods

Male Sprague-Dawley rats (Harlan, Indianapolis, IN, USA) weighing 225–250 g were used in accordance with guidelines mandated in the National Institutes of Health Guide for the Care and Use of Laboratory Animals. The rats were housed on a 12 hr light-dark cycle either singly or in groups of four until surgeries were performed or habituation to experimental conditions was begun, after which all were singly housed. Rats used in cocaine self-administration experiments (see below) were habituated to a 12h reverse light-dark cycle. Access to food and water was provided ad libitum to all rats throughout the study. Unless stated otherwise, chemicals were purchased from Sigma Chemical Company (St. Louis, MO).

Stimulation of RMTg Fos expression

Rats that have self-administered cocaine (about 20 mg/kg/session, at 500 μg/kg per 30 μl infusion), via intravenous catheters for one or six consecutive daily two hours sessions, exhibit striking Fos expression in the RMTg, as do rats given intravenous infusions of investigator-administered cocaine (Geisler et al., 2007b; Marinelli et al., 2008). Furthermore, i.p. injections of methamphetamine (10 mg/kg) given 2 h prior to sacrifice also produce Fos expression in the RMTg (Colussi-Mas et al., 2007; Zahm, unpublished). In view of these findings, sections showing Fos expression in the RMTg in the present study

[1]T.C. Chou and T.C. Jhou, as cited in this paper, identify the same individual (the first author of the paper), the spelling of the name having been changed for phonetic reasons.

came from rats that received intravenous cocaine infusions (as in Geisler et al., 2007b) or methamphetamine injections (as described above).

Tracer injections

Several minutes after being given intraperitoneal injections of a cocktail, consisting of 45% ketamine (100mg/ml), 35% xylazine (20mg/ml) and 20% physiological saline at a dose of 0.16 ml/100g of body weight, rats were placed into a Kopf stereotaxic instrument. The skulls were exposed and small bore holes were created to allow selected brain structures to be targeted by filament-containing borosilicate glass pipettes (O.D. - 1.0 mm) pulled to tip diameters of 10–25 μm and containing the retrograde tracers Fluoro-Gold (FG; Fluorochrome, Inc., Englewood, CO; 1% in 0.1M cacodylate buffer, pH 7.4) or cholera toxin B subunit (CtB, List Biological Laboratories, Campbell, CA), or the anterograde tracer *Phaseolus vulgaris*-leucoagglutinin (PHA-L; Vector, Burlingame, CA, 2.5% in 0.01 M phosphate buffer). A silver wire inserted into the pipettes contacted the solution containing the tracer, which was ejected into the brain substance using positive current pulses (7 s on, 7 s off, for 15 minutes) of 1 μA (for FG) or 4 μA (for PHA-L and CtB). After surgery the rats were kept warm until they awakened.

The results of the study are based upon the evaluation of cases in which injections of FG (3 cases), CtB (2 cases) or PHA-L (4 cases) were centered in the RMTg. Five cases in which PHA-L sites were centered in the LHb were also studied. In addition, ten, six, and eleven cases were evaluated in which FG, CtB and PHA-L injections, respectively, partially involved the RMTg but more substantially invaded adjacent structures. In addition, numerous control retrograde labeling cases were drawn from archived series of injections targeting the retrorubral field (18 cases), pedunculopontine tegmental nucleus (17 cases), laterodorsal tegmental nucleus (17 cases) and ventral tegmental area (49 cases). Structures labeled following injections of retrograde tracers into the RMTg were validated to the extent possible with available archived cases with PHA-L injections in, e.g., the prefrontal cortex, accumbens, ventral pallidum, lateral preoptic area, lateral hypothalamus, ventral tegmental area and substantia nigra compacta. Targeting of injections was done with the aid of stereotaxic coordinates which were initially acquired from the atlas of Paxinos and Watson (1998) and refined empirically. Most abbreviations used in the text, figures and tables also are from Paxinos and Watson (1998).

Fixation of brains and immunocytochemistry

Three days after FG injections and ten days after PHA-L injections, the rats were deeply anesthetized (as above) and perfused transaortically, first with 0.01 M Sorensen's phosphate buffer (SPB; pH 7.4) containing 0.9% sodium chloride and 2.5% sucrose, followed by 0.1 M SPB (pH 7.4) containing 4% paraformaldehyde and 2.5% sucrose. The brains were removed, postfixed, infiltrated with 25% sucrose and sectioned at 50 μm. Five adjacent series of sections were collected, with each thus reflecting the structure of the entire brain from frontal pole to caudal medulla in sections spaced at intervals of 250 μm. Each series of sections was stored in a separate glass vial at −20° C in a cryoprotectant consisting of SPB containing 30% sucrose (by weight) and 30% ethylene glycol (by volume).

One series of sections from each case was immersed in SPB containing 0.1% Triton X-100 (SPB-t) and polyclonal antibodies raised against the relevant tracer, i.e., either anti-FG made in rabbit and used at a dilution of 1:5000, anti-CtB made in goat and used at a dilution of 1:5000, or anti-PHA-L made in goat used at a dilution of 1:10,000. The following day, after thorough rinsing in SPB-t, the sections were immersed for an hour in SPB-t containing biotinylated antibodies made in donkey against rabbit (for FG) or goat IgGs (for PHA-L and CtB) at a dilution of 1:200 (Jackson ImmunoResearch Laboratories Inc., West Grove, PA).

Afterward, the sections were rinsed in SPB and then immersed in SPB containing avidin-biotin-peroxidase complex (ABC - Vector Laboratories, Burlingame, CA) at a dilution of 1:200, also for an hour. After more thorough rinsing in SPB, the sections were immersed for 20–30 min in 0.05 M SPB (pH 7.4) containing 0.05% DAB, 0.04% ammonium chloride, 0.2% β-D-glucose, and 0.0004% glucose oxidase, which generates an insoluble brown reaction product, or, if the sections were destined to be reacted with a second primary antibody, in 0.025 M Tris buffer (pH 8.0) containing 0.015% 3,3'–diaminobenzidine (DAB), 0.4% nickel ammonium sulfate and 0.003% hydrogen peroxide, which generates an insoluble black reaction product.

Sections intended for additional immunohistochemical processing were then further rinsed in SPB and immersed in SPB-t containing anti-c-Fos (Fos), anti-nitric oxide synthase (Nos), anti-myu-mu opioid receptor 1A (Mor), or anti-somatostatin (Som), all made in rabbit, or anti-tyrosine hydroxylase (TH) made in mouse, all used at a dilution of 1:5000. The following morning the sections were rinsed in SPB-t and immersed for one hour in SPB-t containing a donkey antibody against mouse or rabbit IgGs, as appropriate, each used at a dilution of 1:200 (Jackson). Following further rinsing in SPB the sections were immersed for one hour in SPB containing, respectively, mouse or rabbit peroxidase-anti-peroxidase (PAP) at a dilution of 1:3000 (MP Biomedicals, Solon, OH), after which they were again rinsed thoroughly. Then the sections were immersed for 20–30 min in 0.05 M SPB (pH 7.4) containing 0.05% DAB, 0.04% ammonium chloride, 0.2% β-D-glucose, and 0.0004% glucose oxidase (brown reaction product) and, after rinsing, mounted onto gelatin coated slides, dehydrated through a series of ascending concentrations of ethanol, transferred into xylene, and coverslipped with Permount (Fisher, Pittsburgh, PA).

Synthesis and labeling of probes

cDNA probe containing a 593 bp coding sequence for glutamate decarboxylase 67 kD (GAD) [MASST PSPAT SSNAG ADPNT TNLRP TTYDT WCGBA HGCTR KLGLK ICGFL QRTNS LEEKS RLVSA FRERQ ASKNL LSCEN SDPGA RFRRT ETDFS NLFAQ DLLPA KNGEE QTVQF LLEVV DILLN YVRKT FDRST KVLDF HHPHQ LLEGM EGFNL ELSDH PESKE QILVD CRDTL KYGVR TGHPR FFNQL STGLD IIGLA GEWLT STANT NMFTY EIAPV FVLME QITLK KMREI IGWSN KDGDG IFSPG GAISN MYSIM AARYK YFPEV KTKGM AAVPK LVLFT SEHSH YSIKK AGAAL GFGTD NVILI KCNER GKIIP ADLEA KILDA KQKGF VPLYV NATAG TTVYG AFDPI QEIAD ICEKY NLWLH VDAAW GGGLL MSRKH RHKLS GIERA NSVTW NPHKM MGVLL QCSAI LVKEK GILOG CNQMC AGYLF QPDKQ YDVSY DTGDK AIQCG RHVDI FKFWL MWKAK GTVGF ENQIN KCLEL AEYLY AKIKN REEFE MVFNG EPEHT NVCFW YIPQS LRGVP DSPER REKLH RVAPK IKALM MESGT TMVGY QPQGD KANFF RMVIS NPAATQ SDIDF LIEEI ERLGQ DL] was generously provided to Zahm by A. J. Tobin (UCLA) and Jhou by N. Tillakaratne (UCLA). The probes were prepared from a nearly full-length-cDNA clone (3.2 Kb) isolated from a rat brain library and inserted into the bluescript (SK polylinker, Stratagene, La Jolla, CA) EcoRI site (Erlander et al., 1991). Separate clones containing the cDNA insert in different orientations allowed sense and anti-sense probes to be transcribed. Plasmids were incorporated by heat shock into ampicillin-resistant *Escherichia coli* cells, from which templates were isolated and then linearized with *Sal I*. Digoxigenin-labeled or ^{35}S-radiolabeled probes were transcribed with T3 RNA polymerase and were hybridized and detected using, respectively, non-isotopic immunohistochemistry (Geisler et al., 2007a) or photographic emulsion (Marcus et al., 2001; Simmons et al., 1989).

Non-isotopic hybridizations combined with immunohistochemical detection of GAD 67

These were done with free-floating vibratome sections from brains perfused as described above. Diethylpyrocarbonate (DEPC)-treated water was used for all solutions and modifications were applied to methods described by Young (1990). Selected series of sections from operated rats were removed from the freezer and brought to room temperature, after which they were rinsed three times for 10 minutes in SPB. The sections were next immersed in an aqueous 1% solution of sodium borohydride for 15 minutes and then rinsed in SPB every 5 minutes until bubbles were gone. Next, the sections were immersed for 15 minutes in a solution containing triethanolamine, hydrochloric acid and acetic anhydride, after which they were placed for 15 minutes at 55° C in a hybridization buffer consisting of Tris-HCl (20 nM, pH 7.4), EDTA (1 mM), NaCl (300 mM), formamide (50 %), dextran sulfate (10 %), and Denhart's soution (1×). The sections were then placed overnight at 55°C in a mixture consisting of stock probe preparation, nucleic acid mix [salmon sperm DNA (10 μg/ml), yeast total RNA (25 μg/ml), yeast tRNA (25 μg/ml)], sodium dodecyl sulfate (10 %) and sodium thiosulfate (10 %) in hybridization buffer. The dH2O, probe, and nucleic acid mix were first heated to 65°C for 5 minutes, cooled on ice for 5 minutes, and then mixed with the other reagents and brought to 55°C before the sections were added.

Following the hybridization, the sections were thrice rinsed in 4× SSC for 5 minutes at room temperature, 1X SSC three times for 5 minutes at room temperature, 0.1× SSC once for 10 minutes at 65°C and finally cooled to room temp in 0.1X SSC for one minute. The sections were then rinsed in 0.1M Tris-HCl/0.15M NaCl (pH 7.5) for 5 minutes.

Immersion of the sections in 0.1M Tris-HCl containing 0.15M NaCl, 0.3% Triton (pH 7.5) and 0.3 % normal goat serum for 30 minutes preceded overnight immersion at room temperature in the same solution to which had been added mouse anti-digoxigenin antibody-alkaline phosphatase conjugate (Dig, Roche Diagnostics Corporation, Indianapolis, IN), at a dilution of 1:1000, and rabbit anti-FG antibody, at a dilution of 1:5000 (Chemicon). This was followed by two 5 minutes rinses and reaction with reagents comprising an alkaline phosphatase substrate kit VI (Vector) for 2–5 hours in the dark. After an acceptable intensity of GAD 67 mRNA hybridization reaction product had been achieved, the sections were again rinsed in the same buffer and then immersed in SPB-t (pH 7.4) for fifteen minutes. The sections were then placed at room temperature in SPB containing biotinylated anti-rabbit at a dilution of 1:200 for 2 hours, after which they were rinsed three times for 5 minutes in SPB and then further incubated in SPB containing avidin-biotin-horseradish peroxidase conjugate (Vector) for two hours at room temperature. Further rinsing in SPB (three times at 10 minutes) preceded incubation in DAB substrate solution (as above) for 15 minutes followed by three 5 minute rinses in cold SPB. The sections were then mounted from dilute SPB onto glass slides that were then coverslipped with Permount (Fisher).

Hybridizations with ^{35}S-radiolabeled GAD-67 probe combined with immunohistochemical detection of CtB

Free-floating sections were incubated overnight at room temperature in goat anti-CtB (List Biological Laboratories) at a 1:5,000 dilution in PBS with 0.25% Triton X-100 (PBT) and 0.01% sodium azide (Sigma). After the primary incubation, the sections were rinsed three times for 1 min in PBS, incubated in biotinylated donkey anti-goat IgG (Jackson) at a dilution of 1:1000 for 1 hour, rinsed three times for 1 min in PBS, and then incubated in streptavidin-conjugated CY3 (Jackson) at a dilution of 1:1000 for 30 minutes. The sections were then rinsed in PBS and mounted on gelatin-coated glass slides. All reagents were made using water treated with diethylpyrocarbonate (Sigma) to inactivate endogenous RNAse enzymes. Control experiments in which primary antibodies were omitted, or in which tissue

was obtained from rats without CtB injections, resulted in no immunoreactivity above background levels, thus indicating specificity of immunostaining.

The mounted sections were air-dried, and stored in desiccated boxes at −20°C. Prior to the hybridizations, the slides were dehydrated in ascending dilutions of ethanol, cleared in xylenes for 15 minutes, and then rehydrated in descending dilutions of ethanol. To facilitate probe penetration, the slides were placed in sodium citrate buffer (pH 6.0) and heated in a microwave oven (1100 watts) for 10 minutes at 70% power (temperature of 95–100°C). The slides were then dehydrated in ascending dilutions of ethanol and air-dried. The cRNA probe was diluted to 100 cpm/ml in a hybridization solution consisting of 50% formamide, 10 mM Tris-HCl, pH 8.0, 5.0 mg tRNA (Boehringer-Mannheim, Indianapolis, IN), 10 mM dithiothreitol, 10% dextran sulfate, 0.3 M NaCl, 1 mM EDTA at pH 8, and Denhardt's solution (Sigma). Hybridization solution and a coverslip were applied to each slide, and the sections were incubated for 12–16 hours at 57°C. The coverslips were then removed and the slides were washed with sodium chloride/sodium citrate buffer (SSC, pH 7.0). The sections were then incubated in 0.002% RNAase A (Boehringer-Mannheim) with 0.5 M NaCl, 10 mM Tris-HCl, pH 8, and 1 mM EDTA, for 30 minutes and again rinsed in decreasing concentrations of SSC containing 0.25% dithiothreitol (DTT): 2× at 50°C for 1 hour, 0.2× at 55°C for 1 hour, and 0.2× for 1 hour at 60°C. The sections were next dehydrated in graded ethanols (50, 70, 80, and 90%) containing 0.3 M ammonium acetate followed by 100% ethanol and then air-dried and placed in X-ray film cassettes with BMR-2 film (Kodak, Rochester, NY) overnight. The following day the slides were dipped in NTB2 photographic emulsion (Kodak), dried, and stored with desiccant in foil-wrapped slide boxes at 4° C for 4 days. The exposed emulsion was developed with D-19 developer (Kodak).

Combined CtB immunolabeling and GAD 67 hybridizations - data analysis

CtB immunolabeling, visualized under epifluorescence illumination, and silver grains representing GAD 67 hybridization, visualized under darkfield illumination, were photographed using a 25× objective (Zeiss) and a digital camera (Nikon), allowing offline analysis without excessive bleaching of fluorescence. Insofar as CtB immunohistochemistry was performed on floating sections, allowing antibodies to penetrate equally into both tissue surfaces, but in situ hybridization was carried out after the sections had been mounted, GAD 67 mRNA-hybridized neurons occupied preferentially the exposed surface of the sections. Accordingly, CtB immunolabeling was photographed twice for each region of interest, once with the focal plane at the exposed tissue surface, and a second time with the focal plane at the interface of the tissue surface and the glass slide. Co-localization of CtB with GAD 67 was recorded only for CtB neurons appearing more sharply in photomicrographs shot at the exposed surface. CtB-immunoreactive neurons were regarded as expressing GAD 67 if the density of overlying silver grains was more than three times the density observed over non-GABAergic tissue regions in the same section.

Descriptions of Antibodies

anti-Fos—The rabbit polyclonal antibody used to detect Fos was raised against a synthetic peptide corresponding to amino acids 4–17 of human c-Fos. Formerly sold by Oncogene Science (Cambridge, MA) as anti-c-Fos [Ab-5] [4–17] rabbit pAb, it is now supplied (catalogue # PC38) by Calbiochem, a division of EMD Biosciences (San Diego CA). It was raised against the synthetic peptide SGFNADYEASSSRC corresponding to amino acids 4–17 of human c-Fos, and is reported by the vendor to recognize the ~55 kDa c-Fos and ~62 kDa v-Fos proteins and not cross-react with the ~39 kDa Jun protein.

Anti-Dig—The vendor (Roche, Indianapolis, IN) reports that after immunization with digoxigenin, sheep IgG was purified by ion-exchange chromatography, and the specific IgG

was isolated by immunosorption. Fab fragments obtained by papain digestion were purified by gel filtration, conjugated to the specific label, alkaline phosphatase, and stabilized in buffer. The antibody (Catalogue # 11093274910) is reported by the vendor to show 100% reactivity with digoxigenin and digoxin, but no cross-reactivity with other steroids, such as human estrogens (e.g., estradiol) or androgens (e.g., testosterone). The antibody binds only brain sections containing bound digoxigenin labeled mRNA probes, as in *in situ* hybridization histochemistry.

Anti-FG and anti-CtB—This rabbit polyclonal antibody raised against FluoroGold (FG, hydroxystilbamidine) was purchased as antibody-containing serum without preservative (catalogue # AB153) from Chemicon, now Bioscience Research Reagents, a division of Millipore, located Temecula, CA. The vendor states that AB153 also reacts with aminostilbamidine in frozen, 4% PFA fixed tissues. That against CtB was raised in goat against cholera toxin B subunit and sold by List Biological Laboratories, Inc. (Campbell, CA), who report that the greatest dilution of this antibody which forms an immunopreciptin band against a 0.5 mg/ml solution of cholera toxin B is 1:16, which they report is comparable to prior lots of the preparation. In our hands, sections from brains that have not received FG or CtB injections are devoid of reaction product when processed with AB153 and anti-CtB at a range of dilutions and, in brains that have received injections of the tracers, immunostaining is observed only at the injection sites, in retrogradely labeled neurons (and anterogradely labeled axons in the case of CtB) and, occasionally, microglial cells, which, however, are easily distinguished by morphology from labeled neurons.

Anti-Mor—This rabbit polyclonal antibody (Catalogue # OR-600) was provided by Gramsch Laboratories (Schwabhausen, Germany). According to the vendor, it was raised against a synthetic peptide corresponding to amino acids LENLEAETAPLP at the COOH terminus of μ-opioid receptor subtype myu-MOR-1A. In our hands, the antibody stains rat brain sections in a manner consistent with literature descriptions of the distribution of brain Mor immunoreactivity (e.g., Schulz et al., 1998). Preabsorption with the cognate peptide abolished immunohistochemical staining.

Anti-Nos—This rabbit polyclonal antibody provided in 0.01 M phosphate buffered saline, pH 7.4, containing 15 mM sodium azide (Catalogue # N7155) was supplied by the Sigma Chemical Company (Saint Louis, MO). According to the vendor, it was raised against a synthetic peptide corresponding to amino acids 251–270 (GDNDRVFNDLWGKDNVPVILC) of nitric oxide synthase of rat brain origin conjugated to KLH (Riveros-Moreno et al., 1993), reported by the vendor to be an immunogen sequence highly conserved in human bNos. In our hands, the antibody stains rat brain sections in a manner consistent with literature descriptions of the distribution of brain Nos immunoreactivity (e.g., Rodrigo et al., 1994).

Anti-PHA-L—This goat polyclonal antibody raised against *Phaseolus vulgaris* agglutinin (E+L) was purchased (Catalogue # AS-2224) from Vector Laboratories (Burlingame, CA). According to the vendor, this antibody is produced by hyperimmunizing goats with the pure lectin. Following conventional purification steps, specific antibody was isolated by affinity chromatography on lectin-agarose columns and supplied lyophilized in buffered saline. Sections from brains that have not received PHA-L injections are devoid of reaction product when immunoprocessed with AS-2224 at optimal dilutions and, in brains that have received PHA-L injections, immunostaining is observed only at the injection sites and in anterogradely labeled axons.

Anti-Som—This rabbit polyclonal antibody was raised against synthetic somatostatin (AGCKNFFWKTFTSC) conjugated to keyhole limpet hemocyanin with carbodiimide linker provided by ImmunoStar (Hudson, WI) as a lyophilized powder (Catalogue # 20067). The vendor reports that somatostatin immunostaining was completely abolished by preadsorption with somatostatin, somatostatin 25 and somatostatin 28, but not substance P, amylin, glucagon, insulin, neuropeptide Y or vasoactive intestinal polypeptide. In our hands, the antibody stains rat brain sections in a manner consistent with literature descriptions of the distribution of brain somatostatin immunoreactivity (e.g., Johansson et al., 1984).

Anti-tyrosine hydroxylase (TH)—This mouse monoclonal antibody was raised against tyrosine hydroxylase purified from PC12 cells (Catalogue # MAB318) and purchased from the Bioscience Research Reagents (Chemicon) division of Millipore (Temecula, CA). The antibody is supplied as ascites fluid with 3% BSA and no preservative. According to the vendor, the antibody recognizes an epitope on the outside of the regulatory N-terminus of tyrosine hydroxylase. In a Western blot, the antibody recognizes a protein of approximately 59–63 kDa. It does not react with the following on Western Blots: dopamine-beta-hydroxylase, phenylalanine hydroxylase, tryptophan hydroxylase, dehydropteridine reductase, sepiapterin reductase, or phenethanolamine-N-methyl transferase. In our hands, the anti-TH antibody stains rat brain sections in a manner fully consistent with literature descriptions (e.g., Lindvall and Björklund, 1983; Hökfelt et al., 1984).

Immunohistochemical controls

Staining for all of the antibodies described in this paper was absent when the relevant primary or secondary antibodies, ABC or PAP reagents were omitted. Immunoreactivities against Fos, Mor, Nos and Som were abolished by preadsorption with cognate amino acid sequences listed above in the sections describing the antibodies. Immunostaining with FG, CtB and PHA-L antibodies was eliminated by preadsorption, respectively, with FG, CtB and PHA-L. TH antigen was unavailable. However, specificity of anti-TH, like that of anti-NOS and anti-Som, was supported by the observed distribution of the immunoreactivity in rat brain sections, which is consistent with reports in the literature (see above).

Maps and digital images

Retrograde and anterograde labeling were plotted in representative frontal sections throughout the CNS (excluding spinal cord) with the 20× objective under brightfield optics (Nikon Optiphot) with the aid of the AccuStage digitizing system and MDPlot software (AccuStage™, Shoreview, MN). Digital micrographs were generated with the Nikon Optiphot light microscope and a QICAM *Fast* 1394 cooled color 12-bit digital camera (QImaging, Burnaby, BC, Candada) interfaced to Q Capture software (Q Imaging), which saved the image files in TIFF format. The images were sized and subjected to minor adjustments to brightness and contrast with the aid of Adobe Photoshop (version CS2) software. Plates were constructed with Adobe Illustrator (version CS2) software and, upon completion, exported back to TIFF format.

Results

Mor,Som and Nissl

The RMTg, which is located dorsolateral to the caudal half of the interpeduncular nucleus and in the mesencephalic tegmentum behind it, is reliably represented by a dense accumulation of Fos-ir neurons expressed following various environmental and pharmacological stimuli, such as acute methamphetamine or cocaine administration (Figs. 1 and 2) (see Methods). In addition, dense immunoreactivity against Mor (Fig. 1A–F) and Som (Fig. 1G and H) is visible on cellular processes within the Fos activated cluster,

delineating a nearly identical region to that shown by the Fos immunoreactive population. These immunoreactivities are stronger in the medial part of the RMTg (Figs. 1B–F), suggesting some degree of variation of properties within this structure. The pattern of Nissl staining in the region of the RMTg reflects a heterogeneous cellular composition, comprising small and small mediumsized neurons (Fig. 1I and J), that is similar to the surround. Archived sections processed with antisera against calbindin-D 28kD, parvalbumin, Nos, substance P, neurotensin and various gluR receptor subunits distinguished the RMTg poorly or not at all (data not shown).

Relationship to the VTA and retrorubral field

Fos-ir neurons representing the rostral part of the RMTg intermingle with TH-ir neurons and dendrites comprising the caudal part of the VTA (Fig. 2A and B). The caudal part of the RMTg expands into a region with fewer TH-ir elements located beneath the retrorubral field and behind the VTA (Fig. 2C) and ultimately extends into the medial tegmentum in the rostral pons (Fig. 2D). Fos expression was elicited in the sections shown in Fig. 2A–D by investigator-administered cocaine (see Methods) and was not detected in TH-ir neurons in this or any other preparations examined in the study, indicating that the populations of TH-ir and RMTg neurons are distinct.

GAD 67 mRNA

Processing for non-isotopic *in situ* hybridization with a probe against GAD 67 mRNA reveals a cluster of conspicuously densely labeled neurons in the RMTg (Fig. 2E–H). The size, shape and position of this cluster of GAD-expressing neurons precisely replicates that of the dense cluster of Fos-immunoreactive neurons illustrated in Figs. 1 and 2A–D and shown in several previous publications following various experimental treatments (Scammell et al., 2000; Perrotti et al., 2005; Geisler et al., 2007b). Interestingly, the intensity of the GAD-specific non-isotopic reaction product, like that of immunoreactivity against somatostatin and the μ-opioid receptor, varies within the RMTg, but, in contrast to those markers, is particularly strong in the ventrolateral portion of the structure (Fig. 2E and G).

Following injections of the retrograde tracer CtB into the VTA (Fig. 3), neurons in the RMTg became labeled with the tracer and most of these (74.1±1% mean±SEM, n=3) also exhibited GAD 67 hybridization product (long arrows in Figs. 2H; red dots inside dashed outlines in Fig. 3B–J), while a minority did not (black dots in Fig. 3B–J). A similar percentage of CtB neurons in the RMTg of the contralateral hemisphere (75.1±0.8, n=2) also expressed GAD 67 mRNA. In contrast, labeled midbrain neurons outside the RMTg were much less likely to express GAD 67 mRNA; only 25±1.3% (n=3) of CtB-labeled reticular formation neurons outside the RMTg, 5.7±1.8% (n=3) of labeled dorsal raphe neurons, and 5.2±1.3% (n=2) of labeled pedunculopontine tegmental nucleus neurons expressed GAD 67 hybridization product. Furthermore, the projection is topographically organized such that retrograde tracer injections in the lateral part of the VTA, and encroaching into the substantia nigra pars compacta (Fig. 2H, inset) labeled more lateral parts of the RMTg (Fig. 2), whereas more centrally positioned VTA injections are accompanied by a medial shift in the retrograde labeling in the RMTg (Fig. 3), and even more medial VTA injections label only the most medial portion of the RMTg (data not shown). It is also noteworthy that retrogradely labeled GAD 67-expressing neurons, following VTA injections of retrograde tracer, are spread out over an area of the sections somewhat larger than that occupied by the compact cluster of Fos-ir neurons (Fig. 3).

Afferent connections

Injections of FG centered on the RMTg region produced a fairly consistent pattern of retrograde labeling in numerous brain structures extending from the rostral pole of the

frontal cortex to the medulla. Retrograde labeling from a representative FG injection illustrated in Figure 4I–L (case 08023) is diagrammed in Figure 5 and summarized in Table 1. Significant numbers of retrogradely labeled neurons were observed in much of prefrontal cortex, including the rostral association, prelimbic, infralimbic, dorsal peduncular, orbital and cingulate 1 (previously called medial precentral) and 2 (previously called anterior cingulate) areas (Fig. 5A–H). Subcortical labeling was observed in the lateral septum (Fig. 5E–I), medial septum-diagonal band complex (Fig. 5F–H), accumbens (Fig. 5D–G), ventral pallidum (Fig. 5E–I), lateral and medial preoptic region (Fig. 5H–J), ventral bed nucleus of stria terminalis (Fig. 5I, J), sublenticular region (Fig. 5H–K), lateral and dorsal hypothalamus (Fig. 5K–N), entopeduncular nucleus (Fig. 5L, M), hypothalamic paraventricular nucleus (Fig. 5K), LHb (Fig. 5L–N), thalamic parafascicular nucleus (Fig. 5N, O), zona incerta (Fig. 5M–O), supramammillary nucleus (Fig. 5O), periaqueductal gray (Fig. 5O–T), mammillary nucleus (Fig 5P), ventral lateral geniculate nucleus (Fig. 5O), deep layers of the contralateral superior colliculus (Fig. 5Q–S), VTA (Fig.5Q–S), substantia nigra pars compacta and reticulata (Fig. 5Q, R), red nucleus (Fig. 5R), pedunculopontine tegmental nucleus (Fig. 5S, T), dorsal raphe (Fig. 5S), cuneiform nucleus (Fig. 5T), laterodorsal tegmental nucleus (Fig. 5U), parabrachial nucleus (Fig. 5U) and deep cerebellar nuclei (Fig. 5V). Scattered labeling was observed in the pontine and medullary reticular formation (Fig. 5V–W) with occasional labeling in the nucleus ambiguus (Fig. 5V), nucleus of the tractus solitarius and dorsal vagal complex (Fig 5X). While injections in a number of control sites surrounding the RMTg (Fig. 6) frequently produced retrograde labeling in many of the same structures as did injections in the RMTg, the overall profile of retrograde labeling observed after injections in none of these sites precisely matched that observed after RMTg injections (Table 1).

Nos-ir neurons are prominent in several structures in which retrogradely labeled neurons were observed following FG injections in the RMTg. These include the lateral and dorsal hypothalamus (Figs. 5M and 7C and D), ventral lateral geniculate nucleus (Fig. 5O), supramammillary region (Fig. 5O), dorsolateral column of the periaqueductal gray (Fig. 5S), pedunculopontine and laterodorsal tegmental nuclei (Figs. 5S–T and 7A and B) and the pontomedullary reticular formation (Fig. 5V–X). In all of these structures, a proportion of retrogradely labeled neurons was co-labeled with Nos-IR (Fig. 7A–D). In contrast, a scattering of retrogradely labeled neurons that occupied the substantia nigra compacta and adjacent part of the substantia nigra reticulata following RMTg injections of FG (Figs. 5Q and R and 7E) without exception lacked double-labeling with TH-ir (Fig. 7F). Interestingly, injections of anterograde tracer PHA-L into parts of the VTA-nigral complex that contain labeled neurons following injection of retrograde tracer into the RMTg produced little anterograde labeling in any part of the mesopontine tegmentum except the RMTg, which exhibited moderate anterograde labeling following such PHA-L injections (Fig. 8).

LHb

Following injections of FG into the RMTg, retrogradely labeled neurons were very densely packed in the LHb (Figs. 5K–N and 9A). Accordingly, injections of anterogradely transported PHA-L into the LHb (Figs. 9B and E, insets) resulted in dense, focussed labeling of the ipsilateral RMTg, moderate labeling in the contralateral RMTg (Fig. 9B–F), and notably less labeling in regions just outside of the RMTg. The density of ipsilateral RMTg labeling following LHb injections substantially exceeded that observed in other better known recipients of LHb outputs, including the VTA, dorsal, median and paramedian raphe nuclei and the laterodorsal tegmental nucleus (data not shown). The projection from the LHb to the RMTg was topographically organized such that more lateral injections of PHA-L (Fig. 9B, inset) produced labeling in more lateral parts of the RMTg (Fig. 9B–D) as compared to labeling produced by more medial injection sites (Fig. 9E, F). Injections of PHA-L into

medial parts of the LHb produced strong anterograde labeling of a projection to median and paramedian tegmentum that only involved the medialmost part of the RMTg (Fig. 9E and F).

Efferent connections

Injections of PHA-L centered on the RMTg region produced anterograde labeling in numerous brain structures extending from the rostral pole of the frontal cortex to the medulla. Anterograde labeling from a representative PHA-L injection site illustrated in Fig. 4A–D is diagrammed in Fig. 10. Only a few labeled fibers were observed in the frontal cortex (Fig 10A–C). The dorsal hippocampus, which contained moderate labeling in case 07027 (Fig.10D–F), more typically exhibited only a few labeled fibers. Other labeling in the subcortical forebrain was observed in the ventral pallidum (Fig. 10B and C), diagonal band complex (Fig. 10B), lateral preoptic region (Fig. 10C), thalamic midline and intralaminar cell groups (Fig. 10E–F), lateral hypothalamus (Fig. 10E–G), entopeduncular nucleus (Fig. 10D, E), and parafascicular thalamic nucleus (Fig. 10G, H). Anterograde labeling in the brainstem after PHA-L injections into the RMTg was in general heavier than forebrain labeling and involved the periaqueductal gray (Fig. 10H–N), VTA and SNC (Fig. 10H–L), deep mesencephalic nucleus (Fig. 10J–P), dorsal raphe (Fig. 10M–P), pedunculopontine tegmental nucleus (Fig. 10L–O), laterodorsal tegmental nucleus (Fig. 10O, P), locus ceruleus and subceruleus complex (Fig. 10Q), deep cerebellar nuclei (Fig. 10R), and the pontine and medullary reticular formation (Fig. 10R, S). Indeed, by contrast with the brainstem projections of the RMTg, ascending projections to the forebrain were modest, with the most substantial ones terminating in the lateral preoptic region and lateral hypothalamus (Fig. 10C–F). Labeled ascending and descending projections frequently terminated in structures densely occupied by Nos-ir neurons (e.g., Fig. 10D, H, M–O, R and S).

Although it is not possible to objectively compare projection densities after PHA-L injections with any precision, it nevertheless seems that those to the VTA-nigral complex, which predominate ipsilaterally, but also have a strong contralateral component (Figs. 10I–M, 11 and 12) are among the densest outputs of the RMTg. Consistent with the retrograde labeling data (Figs. 2E–H and 3), anterograde tracer deposits in the lateral part of the RMTg (Fig. 11A, inset) robustly labeled axons projecting to the ipsilateral VTA/SNC and only moderately labeled its contralateral counterparts, whereas projections to the contralateral VTA/SNC were more strongly labeled by injections placed more medially in the RMTg (Fig. 11D–F). PHA-L injections in other tegmental sites did not give rise to such robust labeling in the VTA-SNC (Table 2).

Although not so apparently strong as those from the RMTg to the VTA/SNC, outputs from the RMTg to medial parts of the reticular formation (Figs. 10N–Q and 13C and D), laterodorsal and pedunculopontine tegmental nuclei (Figs. 10L–P and 13C and E), dorsal raphe (Figs. 10M and N), and locus ceruleus and the subcerulear complex (Figs. 10Q and 13F) were nonetheless substantial. The density of projections of the RMTg region to the medial tegmentum declined progressively at more caudal levels of the pons and medulla, but nonetheless remained moderate even at the caudalmost levels examined (Fig. 9X).

Discussion

After the attention of neuroscientists had been captured by the conspicuous cluster of Fos-expressing neurons that characterizes the RMTg following various stimuli described in the Introduction, interest in this structure intensified due its reported GABAergic efferents to the VTA-SNC complex (Chou et al., 2004; Geisler et al., 2007b) and afferents from the LHb (Jhou and Gallagher, 2007). The present experiments confirm that robust axonal projections

to the RMTg originate bilaterally in the LHb (Fig. 9) and that GABAergic projections originating in the RMTg terminate bilaterally in the VTA-SNC with a density that rivals, if not exceeds, that of projections traceable to the VTA-SNC from any other brain structure (e.g., Hallanger et al., 1988; Cornwall et al., 1990; Heimer et al., 1991; Zahm et al., 1996; Geisler and Zahm, 2005). Considered together, these anatomical connections are pregnant with implications for the observed negative regulation of VTA-SNC electrophysiological activity by LHb (Christoph et al., 1986; Shepard et al., 2006; Ji and Shepard, 2007; Matsumoto and Hikosaka, 2007; reviewed in Jhou, 2005, and Geisler, 2008).

In view of the potential functional significance of these neuroanatomical features, it seemed advisable to pursue a better understanding of the neuroanatomical organization of this seemingly special part of the mesopontine tegmentum, particularly insofar as one immediately arising question is whether the RMTg, i.e., the mesopontine rostromedial tegmental “nucleus,” is a nucleus at all. At least two immunohistochemically detectable markers, i.e., against Mor (Fig. 1A–F) and Som (Fig. 1G and H) correspond with remarkable fidelity to the region defined by the aforementioned Fos labeling, which, in addition, is characterized by a particularly robust hybridization histochemistry signal for GAD 67 (Figs. 2E–H and 3). Considered together, these features argue in favor of an underlying nuclear framework. However, a number of other characteristics of the region militate against regarding it as strictly nuclear. First, the Nissl staining pattern shows no characteristic cytoarchitecture accompanying the densely Fos-expressing region (Fig. 1I and J). Second, the pattern of retrograde neuronal labeling observed following injections of tracer in the VTA in rats submitted to conditions that produce RMTg Fos expression is only partially consistent with the existence of a discrete “nucleus”. To wit, while the greatest concentration of neurons exhibiting both Fos immunoreactivity and tracer following such injections coincides with the position of the main Fos-expressing cluster (the RMTg), such “double-labeled” neurons are clearly also present in the surrounding tegmentum in numbers that decline with increasing distance from the main cluster (see Figs. 6 and 7 in Geisler et al., 2007b), as if what we are calling RMTg is but a dense focus representing a larger more diffusely organized structure that invades or interdigitates with surrounding structures. Also following VTA tracer injections, a similar pattern exists for GAD 67-expressing, retrogradely labeled neurons, which are maximally represented in the RMTg, but also present in lesser numbers in the surrounding tegmentum (Fig. 3). The retrograde labeling patterns for neurons double-labeled with CtB and GAD 67 mRNA probe (Fig. 3) and FG and Fos-ir (Geisler et al., 2007b) following VTA tracer injections indicate that the RMTg might be more precisely characterized as comprising a compact part (what we so far have been referring to as the RMTg) and a diffuse part that blends or interdigitates with surrounding elements in the tegmentum. Insofar as other nearby structures, such as the laterodorsal and pedunculopontine tegmental nuclei, also comprise compact and diffuse (dissipata) parts (Rye et al., 1987; Hallanger et al., 1988; Cornwall et al., 1990; Steininger et al., 1992; Inglis and Winn, 1995), but nonetheless have long enjoyed “nuclear” status, it seems concordant at this point in time that the RMTg should be similarly regarded.

Nos-ir is widespread in the CNS and co-localizes with a variety of transmitters in various neural subsystems (Bredt et al., 1991; Vincent and Kimura, 1992) and thus is quite useful for distinguishing structure throughout the neuraxis (e.g., Zahm, 2006). We used Nos-ir as a counterstain in the present investigation for this reason, but observed that RMTg afferents and the terminations of some of its efferents are present in a number of sites that are richly endowed with Nos-ir neurons. Indeed, in most cases where neurons projecting to the RMTg sit among numerous Nos-ir neurons, a significant degree of co-localization of the retrograde tracer and Nos-ir was observed (e.g, Figs. 5 and 7). Where this occurs, we have noted it and included some relevant Nos-ir structures in our diagrams (e.g., Fig. 5K, O and S–X and 10D, N, O, R and S). However, we have not investigated, nor are we aware of studies by others

that shed light on, the functional implications of the co-localization of Nos in RMTg afferents.

RMTg afferents

Abundant and direct cortical inputs to the RMTg arise only in rostral, medial and orbital prefrontal, dorsal peduncular, deep insular and anterior cingulate areas (Fig. 14). While the remaining inputs to the RMTg are subcortical in origin, much of the remaining cortex nonetheless could be related to the RMTg via connections that relay in these subcortical structures.

Most of the cortical areas that project to the RMTg also strongly innervate the ventral striatopallidal system (Brog et al., 1993; Ikemoto, 2007), which the present data indicate projects strongly to the RMTg, mainly via neurons in the accumbens shell and ventral pallidum (Fig. 5E–H). This finding from retrograde tracing was confirmed by some of our archived cases with injections of anterograde tracer in the ventral pallidum and accumbens that exhibit a labeled projection to the ventromedial tegmentum that includes the RMTg (Table 3). The ventral part of the bed nucleus of stria terminalis contained some retrogradely labeled neurons following injections of FG in to the RMTg (Fig. 5I and J), and a few were present in the central nucleus of the amygdala and sublenticular region (Fig. 5J and L), suggesting that the contribution to RMTg input from the extended amygdala *per se* is slight compared to that of ventral striatopallidum. This was confirmed by inspection of archived cases with injections of PHA-L into the bed nucleus of stria terminalis and central nucleus of the amygdala (Table 3). However, innumerable retrogradely labeled neurons occupied the entire length of the lateral hypothalamus following FG injections into the RMTg (Fig. 5K–N), and moderate numbers were present in the hypothalamic paraventricular nucleus (Fig. 5K). Insofar as both of these serve, in part, as extended amygdala output structures and are also integral to its overall circuitry (Alheid and Heimer, 1988), a substantial extended amygdala influence on the RMTg likely exists. Thus, while direct projections from the temporal lobe cortex to the RMTg were not detected, temporocortical connectivity with the RMTg via transmission through the extended amygdala would appear to be potentially strong. Furthermore, abundant temporal lobe connections with the RMTg are reflected in robust basal amygdaloid projections to the ventral striatopallidal system (Kelley et al., 1982; Brog et al., 1993), which, as noted, outputs to the RMTg. The RMTg may also be influenced by the central nucleus of the amygdala via central nucleus projections to the ventrolateral PAG (Hopkins and Holstege, 1978), which in turn provides one of the strongest inputs to the RMTg (Fig. 5S–T).

Direct projections from hippocampus to the RMTg also were not detected in the present study, but hippocampus may nonetheless possess the strongest cortical connectivity with the RMTg, insofar as projections to the RMTg arise in a number of structures that are recipients of robust hippocampal projections, including the lateral septum, accumbens, medial septum-diagonal band complex, perifornical hypothalamus and mammillary body, which contained particularly densely packed retrogradely labeled neurons following injections of tracer in the RMTg (Fig. 5O and P). In addition, the lateral preoptic-rostral lateral hypothalamic area (LPH, Reynolds et al., 2006; Geisler and Zahm, 2006), which ranks among the structures in brain most strongly labeled following injections of FG into the RMTg, receives robust inputs from the lateral septum (Jakab and Leranth, 1995). Together with the lateral septum, LPH comprises the so-called “septal-preoptic” macrosystem (Zahm, 2006; Heimer et al., 2008), which serves as a cortico-subcortical output system serving mainly the hippocampus (Alheid and Heimer, 1988; 1996; Swanson, 2000; Heimer et al., 2008). Furthermore, LPH provides a prominent input to the LHb (Herkenham and Nauta, 1977; Kowski et al., 2008), which, as reported here, projects robustly to the RMTg.

Additional structures providing major descending projections to the RMTg include the thalamic parafascicular nucleus, which is extensively interconnected with the cortex and basal ganglia (van der Werf et al., 2002), zona incerta, which receives inputs from widespread cortical areas (Shammah-Lagnado et al, 1985), the aforementioned LHb (Fig. 9), and, aligned along the interface between the substantia nigra pars compacta and reticulata, a collection of non-dopaminergic, possibly GABAergic, neurons, which, due to their location, might be presumed to convey additional basal ganglia influence to the RMTg (Figs. 5Q and R and 8). In sum, descending projections would appear capable of conveying to the RMTg a spectrum of influences originating throughout the forebrain and much of the cortical mantle.

Brainstem and cerebellar projections to the RMTg are also abundant. Quite dense retrograde labeling consistently occupied the intermediate layers of the contralateral superior colliculus following infusions of tracer into the RMTg (Fig. 5Q–S). This, together with moderate but consistent labeling observed in the retino-receptive ventral lateral geniculate nucleus (Harrington, 1997) and reliable labeling of the deep mesencephalic nucleus subjacent to the medial geniculate nucleus, an area that receives polymodal somatosensory projections (Shammah-Lagnado et al., 1985), suggest that the RMTg is reached by short-latency visual and somatosensory signals. Dense retrograde labeling in the PAG following RMTg injections of retrograde tracer (Fig. 5Q–V) involves striking accumulations of neurons in the dorsal raphe nucleus (Fig. 5S), laterodorsal tegmental nucleus (Fig. 5U), locus ceruleus and nucleus prepositus hypoglossi. Another striking cluster of RMTg-projecting PAG neurons occupies a part of the dorsolateral column of the PAG characterized by a dense cluster of Nos-ir neurons (Fig. 5S, see also Vincent and Kimura, 1992). In addition, robust projections to the RMTg are found in the pedunculopontine tegmental nucleus, most particularly within its dissipated part (Fig. 5T), and in the cuneiform and parabrachial nuclei (Fig. 5T and U). In addition, all injections of retrograde tracer into the RMTg resulted in strong labeling of the deep cerebellar nuclei (Fig. 5V) and the contralateral red nucleus.

A technical caveat; anterograde tracing controls

While several studies have reported no uptake of FG by undamaged fibers of passage (Schmued and Fallon, 1986; Pieribone and Aston-Jones 1988; Schmued and Heimer, 1990), Dado et al. (1990) observed minor uptake of FG by fibers of passage, particularly if tissue necrosis was visible at the injection site (see also the discussion in Brog et al., 1993). In the present study, the tracer was injected with a low (1μA) discontinuous (7 seconds on, 7 seconds off) current to minimize the development of heat and consequent tissue damage near the tips of electrodes (Schmued and Heimer, 1990), and a 1% solution of FG was used, as opposed to a more concentrated solution, which has been shown to cause more tissue damage (Schmued and Fallon, 1986). Despite having taken these precautions, we remain somewhat skeptical that no artifactual uptake by fibers-of-passage occurred following injections of FG into a brainstem site that we know is crisscrossed by innumerable myelinated and unmyelinated ascending, descending and crossing pathways. We accordingly regard retrograde labeling as but tentative proof of an anatomical connection until confirmed by anterograde tracing.

With this consideration in mind, we evaluated cases in which anterograde tracer was injected into some of the structures that were retrogradely labeled by injections of FG into the RMTg. First, a concerted effort was made to verify the projection from the LHb to the RMTg because the existence of such a pathway is central to the manner in which the RMTg might serve as an inhibitory intermediary interposed between the LHb and the VTA-SNC complex. Also, in view of the robust projection from the RMTg to the VTA/SNC complex (to be discussed below), we were particularly interested in a potential reciprocal projection in the form of a collection of retrogradely labeled non-dopaminergic neurons scattered along the SNC/SNR interface following FG injections into the RMTg (Figs 5Q and R and 7E and

F). We thus evaluated some PHA-L injections into the area in which these cells were located. Finally, we have evaluated labeled projections in the vicinity of the RMTg in some cases archived from previous studies (e.g., Zahm et al., 1996; 1999; Geisler and Zahm, 2005) in which anterogradely transported compounds had been injected into structures that were found in the present study to be retrogradely labeled following FG injections into the RMTg (Table 3). All of these injections produced reliable anterograde labeling in the RMTg.

RMTg afferents from the LHb

The present observation of a robust projection from LHb to the RMTg (Fig. 9) coheres well with previous reports in which, following injections in the LHb, conspicuous accumulations of projections labeled with tritiated amino acids (Figs. 3I and J, 8B and C, and 9 in Herkenham and Nauta, 1979) and axon terminals labeled with PHA-L (Figs. 2J–L' in Araki et al., 1988) were shown to occupy the site that we now recognize as the RMTg. The density of the projection from LHb to the RMTg, illustrated in our material (Fig. 9), and that of the papers cited above, exceeds that shown for other more familiar projection targets of the LHb, including the VTA, interpeduncular nucleus, median and paramedian raphe and laterodorsal tegmental region. In addition, and consistent especially with the study of Herkenham and Nauta (1979), we observed a topography in the LHb projection to the mesopontine tegmentum such that injections of tracer into more medial LHb regions produced the most robust anterograde labeling in the median and paramedian tegmentum and involved only the most medial and rostral part of the RMTg, whereas sequentially more lateral injections into the LHb produce labeling in proportionately more lateral and caudal parts of the RMTg, such that most of the LHb projection to the RMTg arises in the lateral half of the LHb. Interestingly, this lateral part of the LHb receives its strong input from the ventral pallidum and entopeduncular nucleus (Herkenham and Nauta, 1977), which suggests that a trans-habenula influence of the ventral and dorsal parts of the basal ganglia, respectively, are conveyed to the RMTg, via the projection from the LHb.

RMTg afferents from the nigral complex

Injections of anterograde tracer into the nigral complex revealed labeled projections of modest density, but conspicuous in terms of how restricted they were within the RMTg (Fig. 8). In considering this projection, one should acknowledge that [1] it is significantly bilateral and [2] neurons giving rise to it are scattered along the entire breadth of the VTA-SNC complex. A single PHA-L injection involves a small portion of these neurons and thus only labels a small part of this apparently highly convergent projection. Thus, it seems reasonable to expect that the projection, considered in sum, provides a quite robust reciprocation of the strong projection from the RMTg to the nigral complex (Fig. 11).

RMTg afferents from other forebrain sites

Table 3 provides a list of several archived cases in which anterograde tracers were injected into sites where sizable accumulations of retrogradely labeled neurons were observed following injections of FG into the RMTg. All produced reliable anterograde labeling in the site now recognized as RMTg. However, in contrast to the injection sites described above, i.e., LHb and the VTA/SNC complex, those listed in Table 3 produced anterograde labeling involving a variety of tegmental sites, including the VTA, RMTg, retrorubral field, paramedian tegmentum, mesencephalic reticular formation, pedunculopontine and laterodorsal tegmental regions, periaqueductal gray and others. Hence, these anterograde tracing data confirm that these structures project to the RMTg, but not in a manner that distinguishes the RMTg from adjacent structures.

Outputs of the RMTg

As noted, projections from the RMTg to the forebrain are relatively meager, involving mainly the lateral hypothalamus, lateral preoptic region and midline-intralaminar thalamic cell groups. In contrast, the RMTg gives rise to massive projections remaining within the mesopontine tegmentum and descending to pontomedullary regions (Fig. 10). Among these, a particularly robust projection distributes bilaterally within the VTA/SNC complex (Figs. 10H–J and 11) with a density that far exceeds that of other mesopontine structures reported to innervate the dopaminergic districts (e.g., Deutch et al., 1988; Hallanger et al., 1988; Cornwall et al., 1990; Vertes et al., 1991; Arts et al., 1996; but see also Ferreira et al., 2008; see also Table 2). Alternatively, the RMTg-VTA/SNC projection appears to be not so much more dense than RMTg inputs to several other structures listed above that give rise to massive ascending "state-setting" projections (Mesulam, 1990; Aston-Jones et al., 1991; 2000), which include the nigral complex, pedunculopontine and laterodorsal tegmental nuclei and median and dorsal raphe nuclei (Anden et al., 1964; 1965; 1966; Fallon et al., 1978; Fallon and Moore, 1978; Lindvall and Björklund, 1983; Björklund and Lindvall, 1984; Swanson, 1982; Deutch et al., 1988; Hallanger and Wainer, 1988; Cornwall et al., 1990; Vertes, 1991; Vertes et al., 1999; Gritti et al., 1997; 2003). Consequently, it would appear that much RMTg output may be aimed at modulating the activity in multiple ascending modulatory projections, although this remains to be demonstrated experimentally.

As likely, the RMTg projections may serve to transmit influences conveyed to it in its highly convergent system of descending afferents to lateral mesopontine structures that organize specific motor functions, such as vocalization (periaqueductal gray, see Fig. 10K–N) and micturition (Barringtons's nucleus, see Fig. 10Q). To wit, the RMTg may link both divisions (lateral and medial) of Holstege's emotional motor system (Holstege 1991; 1992; Holstege et al., 2004) to such premotor circuits. These considerations should not be allowed to obscure the potential importance of another major component of RMTg output aimed at medial parts of the mesopontine and pontomedullary reticular formation. These districts give rise to widespread, diffusely organized descending projections that regulate the "gain" or "level" of motor and sensory, particularly nociceptive, transmission throughout the spinal cord (Holstege 1991; 1992; Holstege et al., 2004). Holstege and colleagues, make the interesting point that depression of spinal cord motor function by such pathways might underlie the perceived intractable "tiredness" that accompanies psychomotor depression (Holstege et al., 2004). This phenomenon must now be considered in the light of the massive input to the RMTg from the LHb, a structure with major involvement in depression (reviewed in Geisler and Trimble, 2008).

Functional considerations

Despite the preceding speculations, knowledge about the function of the RMTg is presently limited to findings mentioned in the Introduction. First, lesions involving the RMTg are accompanied by modest hyperactivity and marked reductions of freezing behaviors associated with fear and anxiety (Chou et al., 2004; Jhou, 2005) and Fos expression is elicited in the RMTg by footshock and conditioned stimuli associated with footshock (Jhou and Gallagher, 2007). These findings lead to speculation that the RMTg may be responsible for inhibition of dopamine neuron activity reported to accompany aversive stimuli (Coizet et al., 2006; Ungless et al., 2004; see also Jhou, 2005). Second, psychostimulant drugs robustly elicit Fos expression in the RMTg (Scammell et al., 2000; Geisler et al., 2007b), which leads to the idea that the RMTg may contribute to maintaining dopamine neuron activity in the condition of a drug-elicited increase in extracellular dopamine concentrations (Geisler et al., 2007b). This thought, however, is somewhat at odds with the observation that the VTA-projecting neurons of the RMTg are prominently GABAergic and would thus be expected to inhibit rather than facilitate the activity of targeted neurons. In fact, injections of the GABA

agonist muscimol in the vicinity of the RMTg cause marked increases in accumbens dopamine metabolites, suggesting that inhibition of the RMTg disinhibits dopaminergic accumbens-projecting neurons (Wirtshafter et al., 1988).

All of these considerations and speculations remind us that it remains to be determined if GABAergic neurons in the RMTg that project to the VTA also express Fos-ir following any of the behavioral or pharmacological stimuli so far evaluated; i.e., is it the GABAergic VTA-projecting neurons that are excited by these stimuli? While we have not examined co-localization of GAD 67 with psychostimulant-induced Fos expression, we did observe that, of the RMTg neurons that are retrogradely-labeled following tracer injections in the VTA, a substantial majority expresses GAD 67 (Fig. 3). We also observed in a previous study that a majority of RMTg neurons retrogradely labeled from the VTA express Fos after psychostimulant administration (Geisler et al., 2007b). Thus, it is likely that some RMTg neurons simultaneously express all three indicators: psychostimulant-induced Fos, retrograde label, and GAD67 mRNA. However, the possibility that VTA-projecting GABAergic neurons and VTA-projecting Fos-ir neurons comprise distinct subpopulations of RMTg neurons has not been ruled out at present.

Perspective

Manifold experimental studies done during the nineteenth and early twentieth century in a variety of adult vertebrates, including salamanders, lizards, rats, rabbits, cats and dogs (reviewed in Ferrier, 1876/1966; Hinsey et al., 1930; Bard and Macht, 1958), established that complete transection of the neuraxis at the rostral edge of the mesencephalon, when accompanied by adequate postoperative support, leaves postural reflexes and motor capacity intact. Despite the integrated and coordinated appearance of the locomotion observed following such lesions, however, it nonetheless was regarded as an essentially automaton-like arousal response lacking stimulus-appropriate purpose. Transections at progressively more caudal mesopontine levels rendered animals moribund and incapable of mounting other than fragmented, ineffectual motor-like rhythms. On the basis of these early studies, it was concluded that the mesencephalon and rostral pons comprise an interface where signals descending from the forebrain interact with brainstem motor effectors in the service of adaptive motor function (Harris, 1958).

Classic investigations around the same time period (Moruzzi and Magoun, 1949) indicated that the brainstem reticular formation, particularly in the vicinity of the mesopontine tegmentum (see Shammah-Lagnado et al., 1983), also provides essential contributions to cortical arousal mechanisms. Mesopontine tegmental involvement in the transition between various stages of the sleep-wake cycle also has been oft reported (Aston-Jones and Bloom, 1981; Kayama et al., 1992; Kubin, 2001; Wu et al., 2004), although the triggers are presently thought to reside in the hypothalamus (Saper et al., 2001; 2005; Lu et al., 2006). A “mesopontine tegmental anesthesia area” has been described within which small injections of pentobarbital or muscimol induce deep anesthesia (Devor and Zalkind, 2001; Voss et al., 2005, Sukhotinsky et al., 2007). Moreover, the catecholaminergic, indoleaminergic, cholinergic and GABAergic ascending modulatory, i.e., “state-setting”, projections largely arising in the mesopontine tegmentum (references given above) contribute to fine tuning of forebrain mechanisms in a state-appropriate manner (Mesulam, 1990; Aston-Jones et al., 1991; 2000).

This paper identifies a previously unappreciated structure in the medial mesopontine tegmentum that appears well positioned to be a particularly important player in this milieu. The RMTg may integrate multiple, convergent forebrain and brainstem influences in relation to the dominant LHb and, to a lesser extent, nigral inputs and, in turn, modulate both ascending and descending outputs, possibly in response to fear-arousing and anxiogenic

stimuli, particularly. Via its abundant local connections within the midbrain and rostral pons, the RMTg may profoundly influence various functions "localized" to other nearby sites. In addition, the RMTg may have some, to be determined, role in mediating the behavioral activation elicited by psychostimulant drugs.

Acknowledgments

Grant support: USPHS grants NIH NS-23805, HL-60292 and MH-12370

Literature Cited

Alheid GF, Heimer L. New perspectives in basal forebrain organization of special relevance for neuropsychiatric disorders: the striatopallidal, amygdaloid, and corticopetal components of substantia innominata. Neuroscience. 1988; 27:1–39. [PubMed: 3059226]

Alheid, GF.; Heimer, L. Theories of basal forebrain organization and the "emotional motor system". In: Holstege, G.; Bandler, R.; Saper, CB., editors. The Emotional Motor System. Prog Brain Res. Vol. 107. 1996. p. 461-484.

Andén NE, Carlsson A, Dahlström A, Fuxe K, Hillarp NÅ, Larsson K. Demonstration and mapping out of nigro-neostriatal dopaminergic neurons. Life Sci. 1964; 3:523–530. [PubMed: 14187491]

Andén NE, Dahlström A, Fuxe K, Larsson K. Mapping out of catecholaminergic and 5-hydroxtryptamine neurons innervating the telencephalon and diencephalon. Life Sci. 1965; 4:1275–1279. [PubMed: 5849269]

Andén NE, Dahlström A, Fuxe K, Larsson K, Olson L, Ungerstedt U. Ascending monoamine neurons to the telencephalon and diencephalon. Acta Physiol. Scand. 1966a; 67:313–326.

Araki M, McGeer PL, Kimura H. The efferent projections of the rat lateral habenular nucleus revealed by the PHA-L anterograde tracing method. Brain Res. 1988; 441:319–330. [PubMed: 2451982]

Arts MP, Groenewegen HJ, Veening JG, Cools AR. Efferent projections of the retrorubral nucleus to the substantia nigra and ventral tegmental area in cats as shown by anterograde tracing. Brain Res Bull. 1996; 40:219–28. [PubMed: 8736584]

Aston-Jones G, Bloom FE. Activity of norepinephrine-containing locus coeruleus neurons in behaving rats anticipates fluctuations in the sleep-waking cycle. J Neurosci. 1981; 1:876–886. [PubMed: 7346592]

Aston-Jones G, Rajkowski J, Cohen J. Locus coeruleus and regulation of behavioral flexibility and attention. Prog Brain Res. 2000; 126:165–82. [PubMed: 11105646]

Aston-Jones G, Shipley MT, Chouvet G, Ennis M, van Bockstaele E, Pieribone V, Shiekhattar R, Akaoka H, Drolet G, Astier B, et al. Afferent regulation of locus coeruleus neurons: anatomy, physiology and pharmacology. Prog Brain Res. 1991; 88:47–75. [PubMed: 1687622]

Bard, P.; Macht, MB. The behaviour of chronically decerebrate cats. In: Wolstenholme, GEW.; O'Connor, CM., editors. Ciba Foundation Symposium on the Neurological Basis of Behavior. J & A Churchill, LTD; London: 1958. p. 55-75.

Björklund, A.; Lindvall, O. Dopamine-containing systems in the CNS. In: Björklund, A.; Hökfelt, T., editors. Classical Transmitters in the CNS. Handbook of Chemical Neuroanatomy. Vol. Volume 2. Elsevier; Amsterdam: 1984. p. 55-122.

Bredt DS, Glatt CE, Hwang PM, Fotuhi M, Dawson TM, Snyder SH. Nitric oxide synthase protein and mRNA are discretely localized in neuronal populations of the mammalian CNS together with NADPH diaphorase. Neuron. 1991; 7:615–624. [PubMed: 1718335]

Brog JS, Salyapongse A, Deutch AY, Zahm DS. The patterns of afferent innervation of the core and shell in the "accumbens" part of the rat ventral striatum: immunohistochemical detection of retrogradely transported fluoro-gold. J Comp Neurol. 1993; 338:255–278. [PubMed: 8308171]

Chou TC, Baxter MG, Saper CB. A novel afferent to dopaminergic neurons regulates fear-induced freezing. Soc Neurosci Abstr. 2004; 30:783–13.

Christoph GR, Leonzio RJ, Wilcox KS. Stimulation of the lateral habenula inhibits dopamine-containing neurons in the substantia nigra and ventral tegmental area of the rat. J Neurosci. 1986; 6:613–619. [PubMed: 3958786]

Coizet V, Dommett EJ, Redgrave P, Overton PG. Nociceptive responses of midbrain dopaminergic neurones are modulated by the superior colliculus in the rat. Neuroscience. 2006; 139(4):1479–93. [PubMed: 16516396]

Colussi-Mas J, Geisler S, Zimmer L, Zahm DS, Bérod A. Activation of afferents to the ventral tegmental area in response to acute amphetamine: a double labeling study. Eur. J. Neurosci. 2007; 26:1011–1025. [PubMed: 17714194]

Cornwall J, Cooper JD, Phillipson OT. Afferent and efferent connections of the laterodorsal tegmental nucleus. Brain Res Bull. 1990; 25:271–284. [PubMed: 1699638]

Curran T, Morgan JI. Superinduction of c-fos by nerve growth factor in the presence of peripherally active benzodiazepines. Science. 1985; 229:1265–1268. [PubMed: 4035354]

Dado RJ, Burstein R, Cliffer KD, Giesler GJ Jr. Evidence that Fluoro-Gold can be transported avidly through fibers of passage. Brain Res. 1990; 533:329–333. [PubMed: 1705157]

Deutch AY, Goldstein M, Baldino F Jr, Roth RH. Telencephalic projections of the A8 dopamine cell group. Ann N Y Acad Sci. 1988; 537:27–50. [PubMed: 2462395]

Devor M, Zalkind V. Reversible analgesia, atonia, and loss of consciousness on bilateral intracerebral microinjection of pentobarbital. Pain. 2001; 94:101–112. [PubMed: 11576749]

Erlander MG, Tillakaratne NJK, Feldblum S, Patel N, Tobin AJ. Two genes enconde distinct glutamate decarboxylases. Neuron. 1991; 7:91–100. [PubMed: 2069816]

Fallon JH, Koziell DA, Moore RY. Catecholamine innervation of the basal forebrain. II. Amygdala, suprarhinal cortex and entorhinal cortex. J Comp Neurol. Aug 1; 1978 180(3):509–32. [PubMed: 659673]

Fallon JH, Moore RY. Catecholamine innervation of the basal forebrain. IV. Topography of the dopamine projection to the basal forebrain and neostriatum. J Comp Neurol. 1978; 180:545–80. [PubMed: 659674]

Farvivar R, Zahnenehpour S, Chaudhuri A. Cellular-resolution activity mapping of the brain using immediate-early gene expression. Front Biosci. 2004; 9:104–109. [PubMed: 14766350]

Ferreira JG, Del-Fava F, Hasue RH, Shammah-Lagnado SJ. Organization of ventral tegmental area projections to the ventral tegmental area-nigral complex in the rat. Neuroscience. 2008; 153:196–213. [PubMed: 18358616]

Ferrier, D. The Functions of the Brain. 1876/1966. Smith Elder, London, 1976; reprinted in 1966 by Dawsons of Pall Mall, London

Geisler S, Trimble M. The lateral habenula: no longer neglected. CNS Spectr. 2008; 13:484–489. [PubMed: 18567972]

Geisler S, Derst C, Veh RW, Zahm DS. Glutamatergic afferents of the ventral tegmental area in the rat. J Neurosci. 2007a; 27:5730–5743. [PubMed: 17522317]

Geisler S, Marinelli M, DeGarmo B, Becker ML, Freiman AJ, Beales M, Meredith GE, Zahm DS. Prominent activation of brainstem and pallidal afferents of the ventral tegmental area by cocaine. Neuropsychopharmacol. 2007b advance online publication 19 December 2007; doi: 10.1038/sj.npp.1301650.

Geisler S, Zahm DS. Afferents of the ventral tegmental area in the rat - anatomical substratum for integrative functions. J Comp Neurol. 2005; 490:270–294. [PubMed: 16082674]

Geisler S, Zahm DS. Neurotensinergic afferents of the ventral tegmental area in the rat: [1] re-examination of the origins and [2] responses to acute psychostimulant drug administration. Eur J Neurosci. 2006; 24:116–134. [PubMed: 16882012]

Gritti I, Mainville L, Mancia M, Jones BE. GABAergic and other noncholinergic basal forebrain neurons, together with cholinergic neurons, project to the mesocortex and isocortex in the rat. J Comp Neurol. 1997; 383:163–1. [PubMed: 9182846]

Gritti I, Manns ID, Mainville L, Jones BE. Parvalbumin, calbindin, or calretinin in cortically projecting and GABAergic, cholinergic, or glutamatergic basal forebrain neurons of the rat. J Comp Neurol. 2003; 458:11–31. [PubMed: 12577320]

Hallanger AE, Wainer BH. Ascending projections from the pedunculopontine tegmental nucleus and the adjacent mesopontine tegmentum in the rat. J Comp Neurol. 1988; 274:483–515. [PubMed: 2464621]

Harrington ME. The ventral lateral geniculate nucleus and the intergeniculate leaflet: interrelated structures in the visual and circadian systems. Neurosci Biobehav Rev. 1997; 21:705–727. [PubMed: 9353800]

Harris, GW. Chairman's opening remarks. In: Wolstenholme, GEW.; O'Connor, CM., editors. Ciba Foundation Symposium on the Neurological Basis of Behavior. J & A Churchill, LTD; London: 1958. p. 1-3.

Heimer, L.; Van Hoesen, GW.; Trimble, M.; Zahm, DS. Anatomy of Neuropsychiatry: The New Anatomy of the Basal Forebrain and its Implications for Neuropsychiatric Disease. Elsevier; Amsterdam- New York - San Diego: 2008.

Heimer L, Zahm DS, Churchill L, Kalivas PW, Wohltmann C. Specificity in the projection patterns of accumbal core and shell in the rat. Neuroscience. 1991; 41:89–125. [PubMed: 2057066]

Herkenham M, Nauta WJ. Afferent connections of the habenular nuclei in the rat. A horseradish peroxidase study, with a note on the fiber-of-passage problem. J Comp Neurol. 1977; 173:123–46. [PubMed: 845280]

Herkenham M, Nauta WJ. Efferent connections of the habenular nuclei in the rat. J Comp Neurol. 1979; 187:19–47. [PubMed: 226566]

Hinsey JC, Ranson SW, McNattin RF. The role of the hypothalamus and mesencephalon in locomotion. Arch Neurol Psychiat. 1930; 23:1–42.

Hökfelt, T.; Mårtensson, R.; Björklund, A.; Kleinau, S.; Goldstein, M. Distribution maps of tyrosine-hydroxylase-immunoreactive neurons in the rat brain. In: Björklund, A.; Hökfelt, T., editors. Classical Transmitters in the CNS. Handbook of Chemical Neuroanatomy. Vol. Volume 2. Elsevier; Amsterdam: 1984. p. 277-379.

Holstege G. Descending motor pathways and the spinal motor system: Limbic and nonlimbic components. Prog Brain Res. 1991; 87:307–421. [PubMed: 1678191]

Holstege, GG.; Mouton, LJ.; Gerrits, MN. Emotional motor system. In: Paxinos, G.; Mai, JK., editors. The human nervous system. Elsevier; Amsterdam: 2004. p. 1306-1324.

Holstege G. The emotional motor system. Eur J Morphol. 1992; 30:67–79. [PubMed: 1642954]

Hope BT, Nye HE, Kelz MB, Self DW, Iadarola MJ, Nakabeppu Y, Duman RS, Nestler EJ. Induction of a long-lasting AP-1 complex composed of altered Fos-like proteins in brain by chronic cocaine and other chronic treatments. Neuron. 1994; 13:1235–1244. [PubMed: 7946359]

Hopkins DA, Holstege G. Amygdaloid projections to the mesencephalon, pons and medulla oblongata in the cat. Exp Brain Res. 1978; 32:529–547. [PubMed: 689127]

Ikemoto S. Dopamine reward circuitry: Two projections systems from the ventral midbrain to the nucleus accumbens-olfactory tubercle complex. Brain Res Rev. 2007; 56:27–78. [PubMed: 17574681]

Inglis WL, Winn P. The pedunculopontine tegmental nucleus: where the striatum meets the reticular formation. Prog Neurobiol. 1995; 47:1–29. [PubMed: 8570851]

Jakab, RL.; Leranth, C. Septum. In: Paxinos, G., editor. The Rat Nervous System. Forebrain and Midbrain 2nd Edition. Vol. Volume 1. Academic Press; Sydney: 1995. p. 405-442.

Jhou TC. Neural mechanisms of freezing and passive aversive behaviors. J Comp Neurol. 2005; 493:111–114. [PubMed: 16254996]

Jhou TC, Gallagher M. Paramedian raphe neurons that project to midbrain dopamine neurons are activated by aversive stimuli. Soc Neurosci Abstr. 2007; 33:425, 5.

Ji H, Shepard PD. Lateral habenula stimulation inhibits rat midbrain dopamine neurons through a GABA(A) receptor-mediated mechanism. J Neurosci. 2007; 27:6923–6930. see comment. [PubMed: 17596440]

Johansson O, Hökfelt T, Elde RP. Immunohistochemical distribution of somatostatin-like immunoreactivity in the central nervous system of the adult rat. Neuroscience. 1984; 13:265–339. [PubMed: 6514182]

Kayama Y, Ohta M, Jodo E. Firing of `possibly' cholinergic neurons in the rat laterodorsal tegmental nucleus during sleep and wakefulness. Brain Res. 1992; 569:210–220. [PubMed: 1540827]

Kelley AE, Domesick VB, Nauta WJ. The amygdalostriatal projection in the rat--an anatomical study by anterograde and retrograde tracing methods. Neuroscience. 1982; 7:615–30. [PubMed: 7070669]

Kowski AB, Geisler S, Krauss M, Veh RW. Differential projections from subfields in the lateral preoptic area to the lateral habenular complex of the rat. J Comp Neurol. 2008; 507:1465–1478. [PubMed: 18203181]

Kubin L. Carbachol models of REM sleep: recent developments and new directions. Arch Ital Biol. 2001; 139:147–168. [PubMed: 11256182]

Lindvall, O.; Björklund, A. Dopamine- and norepinephrine-containing neuron systems: Their anatomy in the rat brain. In: Emson, PC., editor. Chemical Neuroanatomy. Raven Press; New York: 1983. p. 229-256.

Lu J, Sherman D, Devor M, Saper CB. A putative flip-flop switch for control of REM sleep. Nature. 2006; 441:589–594. [PubMed: 16688184]

Marinelli M, Geisler S, Becker ML, Freiman AJ, Zahm DS. Profiles of Fos expression elicited in multiple brain structures by self- and investigator-administered cocaine and vehicle after one and six sessions. Soc Neurosci Abstract. 2008; 273(10):2008.

Marcus JN, Aschkenasi CJ, Lee CE, Chemelli RM, Saper CB, Yanagisawa M, Elmquist JK. Differential expression of orexin receptors 1 and 2 in the rat brain. J Comp Neurol. 2001; 435:6–25. [PubMed: 11370008]

Matsumoto M, Hikosaka O. Lateral habenula as a source of negative reward signals in dopamine neurons. Nature. 2007; 447:1111–1115. [PubMed: 17522629]

Mesulam M-M. Large-scale neurocognitive networks and distributed processing for attention, language and memory. Ann Neurol. 1990; 28:597–613. [PubMed: 2260847]

Morgan JI, Cohen DR, Hempstead JL, Curran T. Mapping patterns of c-fos expression in the central nervous system after seizure. Science. 1987; 237:192–197. [PubMed: 3037702]

Morgan JI, Curran T. Role of ion flux in the control of c-fos expression. Nature. 1986; 322:552–555. [PubMed: 2426600]

Moruzzi G, Magoun HW. Brain stem reticular formation and activation of the EEG. Electroencephalogr Clin Neurophysiol. 1949; 1:455–473. [PubMed: 18421835]

Olson VG, Nestler EJ. Topographical organization of GABAergic neurons within the ventral tegmental area of the rat. Synapse. 2007; 61:87–95. [PubMed: 17117419]

Paxinos, G.; Watson, C. The rat brain in stereotaxic coordinates. Fourth edition. Academic Press; San Diego, CA: 1998.

Perrotti LI, Bolaños CA, Choi K-H, Russo SJ, Edwards S, Ulery PG, Wallace DL, Self DW, Nestler EJ, Barrot M. ΔFosB accumulates in a GABAergic cell population in the posterior tail of the ventral tegmental area after psychostimulant treatment. Eur J Neurosci. 2005; 21:2817–2824. [PubMed: 15926929]

Pieribone VA, Aston-Jones G. The iontophoretic application of Fluoro-Gold for the study of afferents to deep brain nuclei. Brain Res. 1988; 475:259–271. [PubMed: 3214735]

Reynolds SM, Bérod A, Geisler S, Zahm DS. Neurotensin antagonist acutely and robustly attenuates locomotion that accompanies stimulation of a neurotensin-containing pathway from rostrobasal forebrain to the ventral tegmental area. Eur J Neurosci. 2006; 24:188–196. [PubMed: 16882016]

Riveros-Moreno V, Beddell C, Moncada S. Nitric oxide synthase: structural studies using anti-peptide antibodies. Eur J Biochem. 1993; 215:801–808. [PubMed: 7689053]

Rodrigo J, Springall DR, Uttenthal O, Bentura ML, Abadia-Molina F, Riveros-Moreno V, Martínez-Murillo R, Polak JM, Moncada S. Localization of nitric oxide synthase in the adult rat brain. Philos Trans R Soc Lond B Biol Sci. 1994; 345:175–221. [PubMed: 7526408]

Rye DB, Saper CB, Lee HJ, Wainer BH. Pedunculopontine tegmental nucleus of the rat: cytoarchitecture, cytochemistry, and some extrapyramidal connections of the mesopontine tegmentum. J Comp Neurol. 1987; 259:483–528. [PubMed: 2885347]

Saper CB, Chou TC, Scammell TE. The sleep switch: hypothalamic control of sleep and wakefulness. Trends Neurosci. 2001; 24:726–731. [PubMed: 11718878]

Saper CB, Scammell TE, Lu J. Hypothalamic regulation of sleep and circadian rhythms. Nature. 2005; 437:1257–1263. [PubMed: 16251950]

Scammell TE, Estabrooke IV, McCarthy MT, Chemelli RM, Yanagisawa M, Miller MS, Saper CB. Hypothalamic arousal regions are activated during modafinil-induced wakefulness. J Neurosci. 2000; 20:8620–8628. [PubMed: 11069971]

Schmued LC, Fallon JH. Fluoro-Gold: a new fluorescent retrograde axonal tracer with numerous unique properties. Brain Res. 1986; 377:147–154. [PubMed: 2425899]

Schmued LC, Heimer L. Iontophoretic injection of Fluoro-Gold and other fluorescent tracers. J Histochem Cytochem. 1990; 38(5):721–723. [PubMed: 2332627]

Schulz S, Schreff M, Koch T, Zimprich A, Gramsch C, Elde R, Höllt V. Immunolocalization of two mu-opioid receptor isoforms (MOR1 and MOR1B) in the rat central nervous system. Neuroscience. 1998; 82:613–22. [PubMed: 9466465]

Shammah-Lagnado SJ, Negrão N, Ricardo JA. Afferent connections of the zona incerta: a horseradish peroxidase study in the rat. Neuroscience. 1985; 15:109–34. [PubMed: 4010931]

Shammah-Lagnado SJ, Ricardo JA, Sakamoto NT, Negrão N. Afferent connections of the mesencephalic reticular formation: a horseradish peroxidase study in the rat. Neuroscience. 1983; 9:391–409. [PubMed: 6877601]

Sharp FR, Sagar SM, Swanson RA. Meabolic mapping wiht cellular resolution: c-fos vs. 2 deoxyglucose. Crit Rev Neurobiol. 1993; 7:205–228. [PubMed: 8221912]

Simmons DM, Arriza JL, Swanson LW. A complete protocol for in situ hybridization of messenger RNAs in brain and other tissues with radiolabelled single stranded RNA probes. J Histotechnol. 1989; 12:169–181.

Shepard PD, Holcomb HH, Gold JM. Schizophrenia in translation: the presence of absence: habenular regulation of dopamine neurons and the encoding of negative outcomes. Schizophr Bull. 2006; 32:417–421. [PubMed: 16717257]

Steininger TL, Rye DB, Wainer BH. Afferent projections to the cholinergic pedunculopontine tegmental nucleus and adjacent midbrain extrapyramidal area in the albino rat. I. Retrograde tracing studies. J Comp Neurol. 1992; 321:515–543. [PubMed: 1380518]

Sukhotinsky I, Hopkins DA, Lu J, Saper CB, Devor M. Movement suppression during anesthesia: neural projections from the mesopontine tegmentum to areas involved in motor control. J Comp Neurol. 2005; 489:425–448. [PubMed: 16025457]

Sukhotinsky I, Zalkind V, Lu J, Hopkins DA, Saper CB, Devor M. Neural pathways associated with loss of consciousness caused by intracerebral microinjection of GABA A-active anesthetics. Eur J Neurosci. 2007; 25:1417–1436. [PubMed: 17425568]

Swanson LW. The projections of the ventral tegmental area and adjacent regions: a combined fluorescent retrograde tracer and immunoflourescence study in the rat. Brain Res Bull. 1982; 9:321–353. [PubMed: 6816390]

Ungless MA, Magill PJ, Bolam JP. Uniform inhibition of dopamine neurons in the ventral tegmental area by aversive stimuli. Science. Mar 26; 303(5666):2040–2. [PubMed: 15044807]

van der Werf YD, Witter MP, Groenewegen HJ. The intralaminar and midline nuclei of the thalamus. Anatomical and functional evidence for participation in processes of arousal and awareness. Brain Res Rev. 2002; 39:107–140. [PubMed: 12423763]

Vertes RP. A PHA-L analysis of ascending projections of the dorsal raphe nucleus in the rat. J Comp Neurol. 1991; 313:643–668. [PubMed: 1783685]

Vertes RP, Fortin WJ, Crane AM. Projections of the median raphe nucleus in the rat. J Comp Neurol. 1999; 407:555–582. [PubMed: 10235645]

Vincent SR, Kimura H. Histochemical mapping of nitric oxide synthase in the rat brain. Neuroscience. 1992; 46:755–784. [PubMed: 1371855]

Wirtshafter D, Klitenick MA, Asin KE. Is dopamine involved in the hyperactivity produced by injections of muscimol into the median raphe nucleus? Pharmacol Biochem Behav. Jul; 1988 30(3):577–83. [PubMed: 3211966]

Wu MF, John J, Boehmer LN, Yau D, Nguyen GB, Siegel JM. Activity of dorsal raphe cells across the sleep-waking cycle and during cataplexy in narcoleptic dogs. J Physiol. 2004; 554:202–215. [PubMed: 14678502]

Voss LJ, Young BJ, Barnards JP, Sleigh J. Differential anaesthetic effects following microinjection of thiopentone and propofol into the pons of adult rats: a pilot study. Anaesth Intensive Care. 2005; 33:373–380. [PubMed: 15973921]

Young, WS, III. Analysis of Neuronal Microcircuits and Synaptic Interactions. In situ hybridization histochemistry. In: Björklund, A.; Hokfelt, T.; Wouterlood, FG.; van den Pol, AN., editors.

Handbook of Chemical Neuroanatomy. Vol. Vol. 8. Elsevier Science Publishers; Amsterdam: 1990. p. 481-511.

Zahm DS. The evolving theory of basal forebrain "functional anatomical macrosystems. Neurosci Biobehav Rev. 2006; 30:148–172. [PubMed: 16125239]

Zahm DS, Jensen SL, Williams ES, Martin JR 3rd. Direct comparison of projections from the central amygdaloid region and nucleus accumbens shell. Eur. J. Neurosci. 1999; 11:1119–1126. [PubMed: 10103108]

Zahm DS, Williams EA, Wohltmann C. The ventral striatopallidothalamic projection: IV. Relative contributions from neurochemically distinct pallidal subterritories in the subcommissural region and olfactory tubercle and from adjacent extrapallidal parts of the rostrobasal forebrain. J Comp Neurol. 1996; 364:340–362. [PubMed: 8788254]

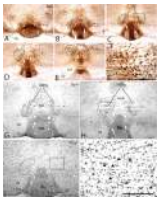

Figure 1.

Photomicrographs illustrating the mesopontine rostromedial tegmental nucleus (RMTg) in preparations processed for μ-opioid receptor 1A (Mor) immunoreactivity (A–F), somatostatin (Som) immunoreactivity (G and H) and Nissl staining (I and J). The rat from which the sections shown in A–F, I and J were taken received an injection of methamphetamine (10 mg/kg) two hours prior to sacrifice in order to elicit the expression in the RMTg of Fos, which is shown as a second immunolabel in A–F (black dots [Fos-ir nuclei], in contrast to Mor-ir, which is brown). Note in panels B–E that strong immunoreactivity against Mor is coextensive with a dense cluster of Fos-immunoreactive nuclei. Note also that Mor-ir is denser in the medial (asterisk in C and F, an enlargement of the box in C) than lateral part of the RMTg. The RMTg is encircled on the left indicated by arrows on the right in A, B, D, E, G and H. Note the location of the RMTg in relation to the interpeduncular nucleus (IPN), medial lemniscus (ml) and the horizontal fascicles of the ventral tegmental (tgx) and superior cerebellar peduncle (xscp) decussations. In G and H, somatostatin immunoreactivity is shown at a rostral (G) and more caudal (H) level of the RMTg. Panel I shows a section adjacent to the one illustrated in C (note similar pattern of vessels in the IPN in C and I) and demonstrates that the RMTg is relatively undistinguished from surrounding regions in Nissl-stained preparations. Arrows in J, which is an enlargement of the boxed area in I, indicate the variety of small and small-medium sized neurons located in the RMTg. Scale bars: 1 mm in A–E, 200 μm in F (bar in F); 1 mm in G–I, 200 μm in J (bar in J).

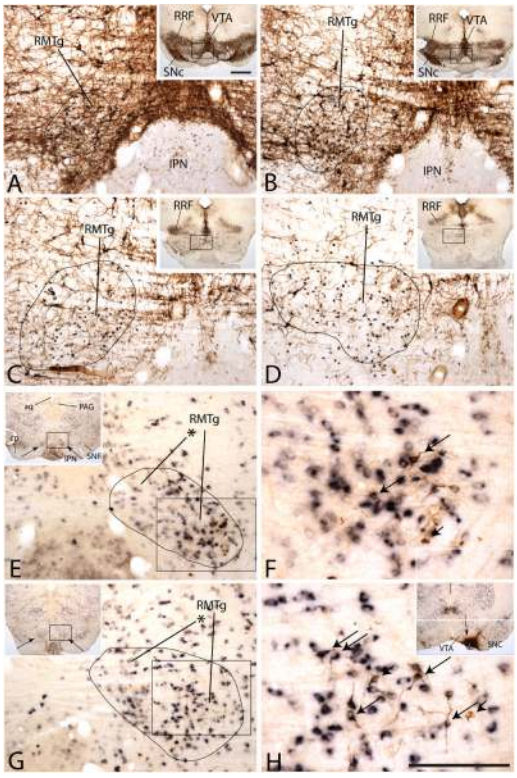

Figure 2.

A–D. Photomicrographs of the rostromedial tegmental nucleus (RMTg, encircled in A–D) at sequentially more caudal levels, illustrating its relationship to tyrosine hydroxylase immunoreactive (TH-ir) elements in the ventral tegmental area (VTA) and retrorubral field (RRF). Note at rostral levels of the RMTg (A and B) that Fos immunoreactive nuclei (black dots) representing the RMTg (Fos expression was elicited by an i.p. methamphetamine injection) are embedded among TH-ir neurons and processes (the brown immunostained elements in the micrographs), which are fewer and more widely scattered at more caudal levels (C and D). The boxed areas in the insets are enlarged in the corresponding panels. E – H. Photomicrographs showing the rostromedial tegmental nucleus (RMTg, encircled in E and G) in sections processed with a cRNA probe against glutamate decarboxylase-67 mRNA (black label). Also shown is the distribution in the RMTg of Fluoro-Gold immunoreactive neurons (brown label) following an injection of retrogradely transported tracer into the ventral tegmental area (arrowed in the inset in H). The RMTg is shown at sequentially more caudal levels in panels E andG, which are enlargements of the boxed areas in the accompanying insets. Boxes in E and G are enlarged in panels F and H, respectively. Note, in panels F and H, that numerous neurons indicated by long arrows exhibit both labels, whereas other RMTg neurons exhibit only the black or brown (short arrows) label. Additional abbreviations: aq - cerebral aqueduct; cp - cerebral peduncle; IPN - interpeduncular nucleus; PAG - periaqueductal gray; SNR and SNC - substantia nigra reticulata and compacta; VTA - ventral tegmental area. Scale bars: 400 μm for A–D, E and G; 200 μm for F and H (bar in H); 1 mm for insets (bar in inset A).

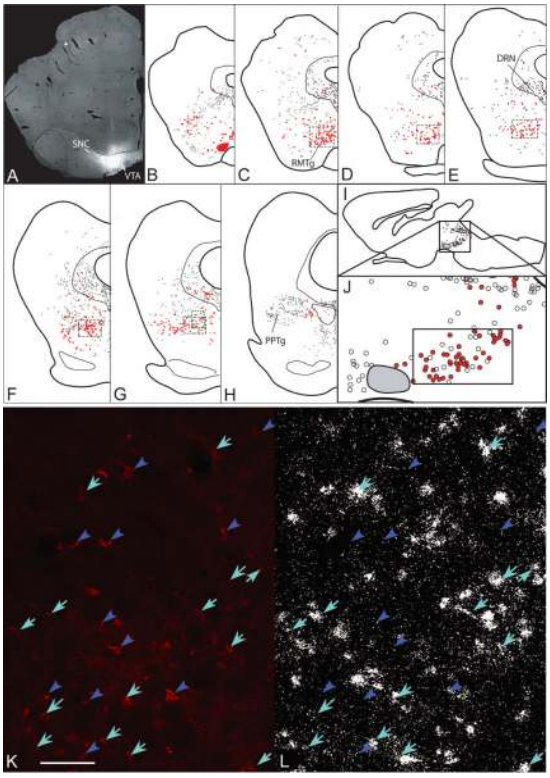

Figure 3.

An injection of CtB into the ventral tegmental area (VTA), shown in a fluorescence micrograph in A, produces many labeled neurons in the midbrain, shown in frontal sections in rostrocaudal sequence (B–H). CtB labeled neurons expressing GAD 67 mRNA are represented by filled red circles, and are particularly enriched in the rostromedial tegmental nucleus (RMTg, boxed in black in C–G), while CtB-labeled neurons lacking GAD67 are represented as filled black dots, and predominate outside of the RMTg. The red spot in panel B represents a region just outside the CtB injection site, where labeled cells and fibers were too dense to identify reliably. A diagrammed sagittal section (I) illustrates that the region of CtB-labeled neurons expressing GAD67 extends caudodorsally from the VTA injection site (grey filled patch). The box in I is enlarged in J, within which the RMTg region is outlined. Panels K and L are photomicrographs of the green boxed area in panel G and are intended to serve as representative of tissue processed to reveal both CtB and GAD67. CtB is indicated by red fluorescent label (K), while GAD67 mRNA is indicated by silver grains (L). CtB neurons expressing GAD67 are indicated by cyan arrows, while those lacking GAD67 are indicated by blue arrowheads. Additional abbreviations: DRN - dorsal raphe nucleus; PPTg - pedunculopontine tegmental nucleus; SNC - substantia nigra compacta. Scale bar: 100μm.

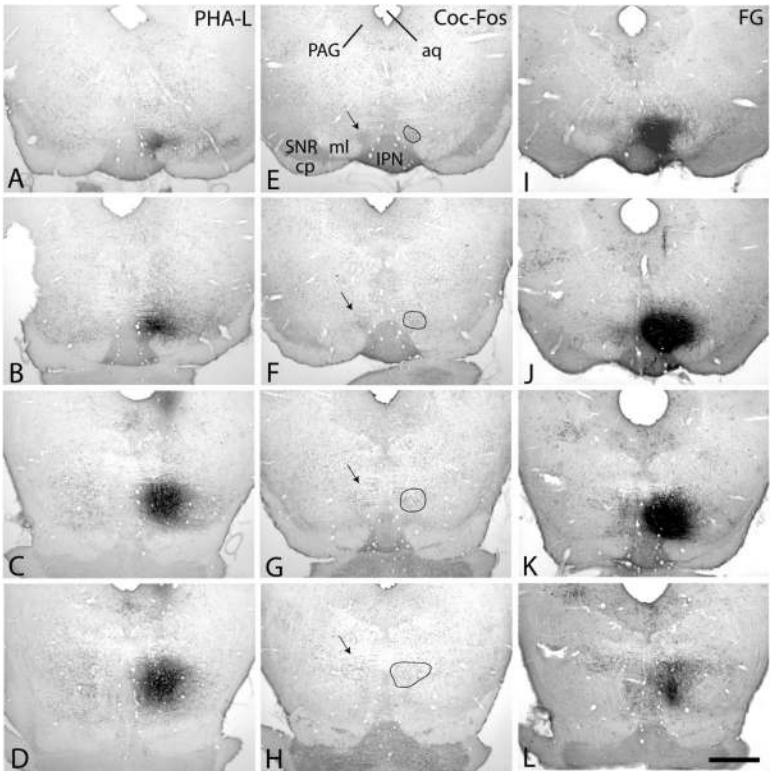

Figure 4.

Photomicrographs illustrating, from top to bottom, four sequentially more caudal transverse sections through the mesencephalon and rostral pons from three cases. Corresponding levels are shown in each horizontal row. The rostromedial tegmental nucleus (RMTg) is encircled in panels E–H, which came from a rat (case 06130) in which Fos expression was elicited in the RMTg by cocaine administration. Sections from that brain were processed to exhibit Fos immunoreactive neurons, which are densely clustered within the RMTg (arrows on left and encircled on right in E–H). The sections shown in panels A–D came from a rat that received an injection of anterogradely transported PHAL (case 07027), while those shown in panels I–L came from a rat that received an injection of retrogradely transported Fluoro-Gold (case 08023), both of which can be seen to occupy the RMTg by reference to panels E–H. Maps illustrating the resulting transport of tracers are shown in Figures 5 (08023) and 10 (07027). Additional abbreviations: aq - cerebral aqueduct; cp - cerebral peduncle; IPN - interpeduncular nucleus; ml - medial lemniscus; PAG - periaqueductal gray; SNR - substantia nigra reticulata. Scale bar: 1 mm.

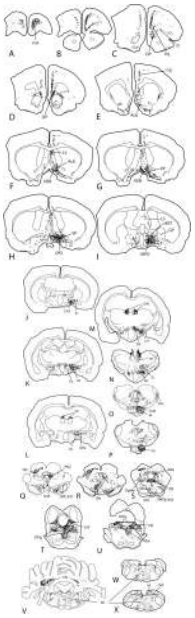

Figure 5.

Map illustrating the distribution in the rat brain of retrogradely labeled neurons following injection of Fluoro-Gold into the medial tegmental nucleus (RMTg). The injection site is shown in Figure 4 I– L. Each dot represents one retrogradely labeled neuron. Selected groups of nitric oxide synthase immunoreactive neurons are indicated as gray dots in selected panels (K, O, and S–X). Abbreviations: 10 -dorsal motor nucleus of the vagus nerve; Acb - nucleus accumbens; Bar - Barrington's nucleus; vBST - bed nucleus of stria terminalis, ventral part; Cg - cingulate cortex; CN - deep cerebellar nuclei; CnF - cuneiform nucleus; DA - dorsal hypothalamic area; DP - dorsal peduncular cortex; DpMe - deep mesencephalic nucleus; DR - dorsal raphe; EPN - entopeduncular nucleus; FrA - frontal association cortex; GP - globus pallidus; IPN - interpeduncular nucleus; ISC - intermediate layers of the superior colliculus; LDTg - laterodorsal tegmental nucleus; LH - lateral hypothalamus; LHb - lateral habenula; LPO - lateral preoptic area; LS - lateral septum; M - mammillary nucleus; MPO - medial preoptic area; O - orbital cortex; Pa - hypothalamic paraventricular nucleus; PAG - periaqueductal gray; PB - parabrachial nucleus; PF - parafascicular nucleus; PH - posterior hypothalamic area; PPTg - pedunculopontine tegmental nucleus; PrL - prelimbic cortex; RN - red nucleus; Rt - reticular formation; SI - substantia innominata; sm - stria medullaris; SNC & R - substantia nigra pars compacta and reticulata; Sol - nucleus of the tractus solitarius; SuM - supramammillary nucleus; VDB - vertical limb of the diagonal band; VLG - ventral lateral geniculate nucleus; RMTg - medial tegmental nucleus; VP - ventral pallidum; VTA - ventral tegmental area; ZI - zona incerta.

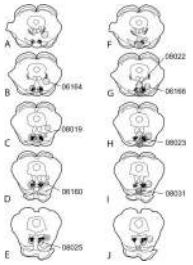

Figure 6.
Maps illustrating Fluoro-Gold injection sites into the RMTg (08019, 08023, and 08025) and into control sites surrounding it (06160, 06164, 06166, 08022, 08031). Panels A–E and F–J are replicate sequences of idealized transverse sections through the mesencephalon and rostral pons at increasingly caudal levels from top to bottom. Four fill-coded injection sites are shown in each series. The RMTg is represented by clustered black dots, which reflect Fos immunoreactive neurons plotted in sections from a rat that received an injection of methamphetamine 2 hours prior to sacrifice. Brain structures in which retrogradely labeled neurons were observed in each indicated case are given in Table 1.

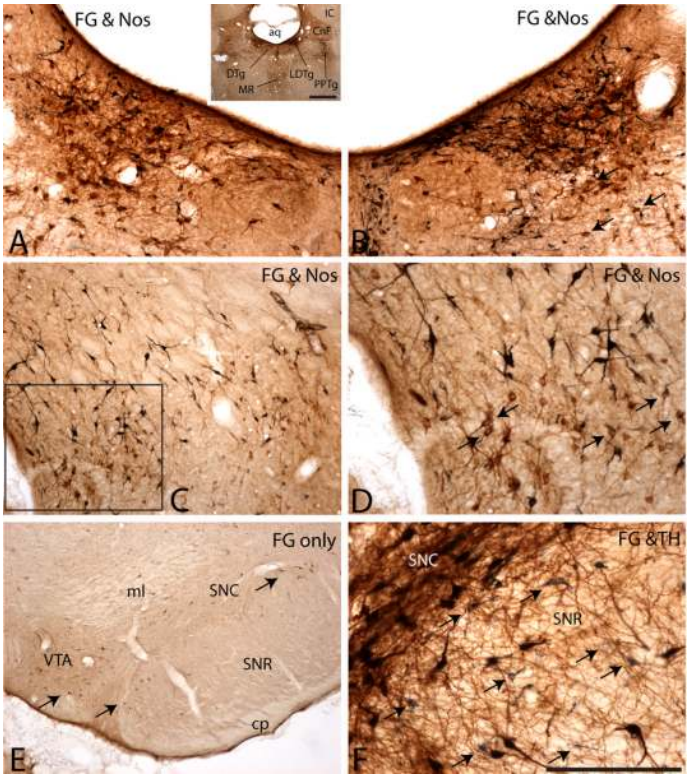

Figure 7.

A sampling of sites where neurons that became retrogradely labeled (black reaction product) following Fluoro-Gold (FG) injections into the rostromedial tegmental nucleus (case 08023) are extensively co-distributed with nitric oxide synthase (Nos, panels A–D) or tyrosine hydroxylase (TH, panels E and F) immunoreactive (ir) neurons. Innumerable retrogradely labeled (black label) and Nos-ir (brown label) neurons occupy the laterodorsal tegmental nucleus (LDTg) ipsilateral to the injection site (B and inset in A) and many of these contain both labels. Fewer retrogradely labeled neurons are present in the contralateral LDTg (A). Likewise, retrogradely labeled (black) and Nos-ir (brown) neurons are extensively intermixed in the ipsilateral lateral hypothalamus (C) and many contain both labels (arrows in D, an enlargement of the box in C). Retrogradely labeled neurons in the ventral tegmental area and substantia nigra are shown in panel E (some examples are arrowed). In panel F, which illustrates a section adjacent to the one shown in E, retrogradely labeled neurons are shown in black (arrows) relative to TH-ir neurons (brown). Neurons exhibiting the retrograde label and TH-ir were not observed. Additional abbreviations: aq - cerebral aqueduct; CnF - cuneiform nucleus; cp - cerebral peduncle; DTg - dorsal tegmental nucleus; IC - inferior colliculus; ml - medial lemniscus; MR - median raphe; PPTg - pedunculopontine tegmental nucleus; SNC & R - substantia nigra pars compacta & reticulata. Scale bars: 400 μm in A–C, 200 μm in D and F, 1mm in E (bar in F); 1 mm in inset A.

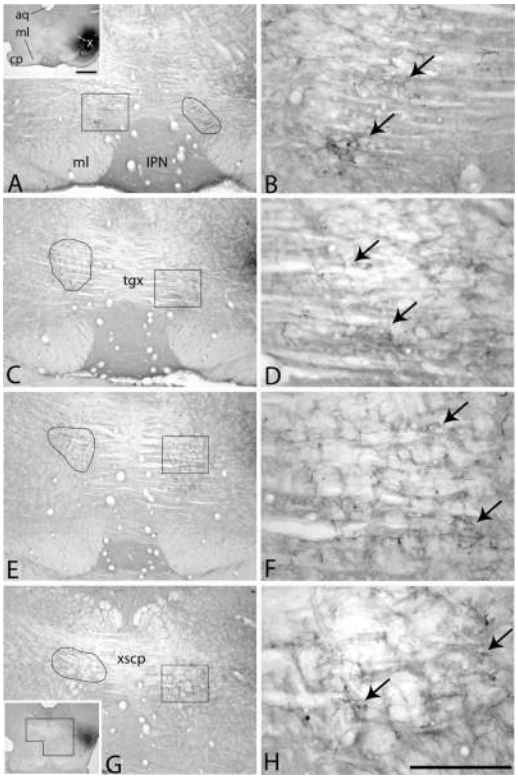

Figure 8.

Photomicrographs illustrating a labeled projection to the ipsilateral and contralateral medial tegmental nucleus (RMTg) observed following injection of PHA-L into the substantia nigra pars compacta and adjacent reticulata (white x in inset in A). Panels A, C, E and G show sequentially more caudal sections through the RMTg (encircled on side, boxed on the other). Note that immunoperoxidase product is present in the boxes in A, C, E, and G, of which all, except the one in A, are ipsilateral to the injection site. B, D, F and H, respectively, are enlargements of the boxes in A, C, E and G and reveal that the labeling in the boxes reflects PHA-L labeled axonal projections. Arrows in A, C, E and G indicate labeling in the RMTg on the side not indicated by a box. Arrows in B, D, F and H indicate some of the labeled axons. Additional abbreviations: aq: cerebral aqueduct; cp - cerebral peduncle; IPN - interpeduncular nucleus; ml - medial leminscus; tgx - tegmental decussation; xscp - decussation of the superior cerebellar peduncle. Scale bars: 1 mm in A, C, E and G; 200 μm in B, D, F and H (bar in H); 1 mm in inset A.

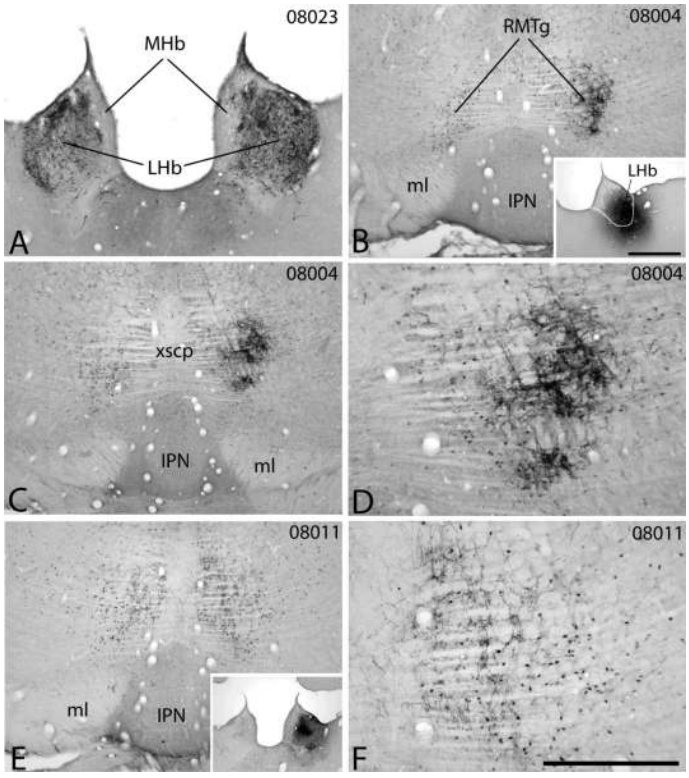

Figure 9.

Photomicrographs illustrating a robust, selective projection from the lateral habenula (LHb) to the medial tegmental nucleus (RMTg). Panel A displays the prominent ipsilateral (right side) and less prominent contralateral distribution of retrogradely labeled neurons in the LHb following an injection of Fluoro-Gold into the RMTg (case 08023, injection site shown in Fig. 4 I–K and 6G–J). Panels B–D illustrate the prominent ipsilateral (right side) and less prominent contralateral distribution of anterogradely labeled fibers in the RMTg following a PHA-L injection into the LHb shown in the inset in B. Panels B and C (case 08004) show more rostral and caudal levels of the RMTg, respectively, and D shows the ipsilateral (right side) labeling in C, enlarged. Rat 08004 was administered 10 mg/kg of methamphetamine 2 hours prior to sacrifice to elicit Fos expression in the RMTg and this is reflected in the black dots [Fos-ir nuclei] shown in panels B–F. Note that the dense anterograde labeling is distributed coextensively with the dense clusters of Fos-ir neurons. Panels E and F (case 08011, also received methamphetamine) illustrate a more medial injection of PHA-L into the LHb (inset in E), which gives rise to anterograde labeling that involves only the medialmost part of the RMTg (see panel F, an enlargement of the ipsilateral anterograde labeling (right side) in panel E. Additional abbreviations: IPN - interpeduncular nucleus; MHb - medial habenula; ml - medial lemniscus; xscp - decussation of the superior cerebellar peduncle. Scale bars: 1 mm in A, B, C, and E, 400 μm in D and F (bar in F); 1mm in insets (bar in inset B).

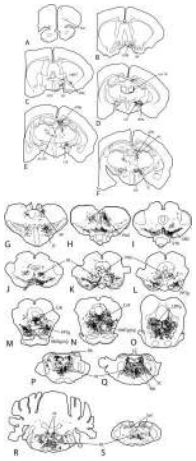

Figure 10.

Map illustrating the distribution in the rat brain of anterogradely labeled fibers following an injection of PHA-L into the rostromedial tegmental nucleus. The injection site is shown in Figure 4A–D. Symbols (pluses) indicate anterograde labeling in numbers that, based upon subjective impression, correspond approximately to the density of labeling observed in the sections. Selected groups of nitric oxide synthase immunoreactive neurons are indicated as gray dots in selected panels (D, H, M, N, O, R and S). The ventral tegmental area (VTA) and substantia nigra compacta (SNC) area outlined in panels I–K. The circumscribed injection site (inj) is indicated in panels M and N. Tyrosine hydroxylase immunoreactive neurons and fibers of the locus ceruleus (LC) and subceruleus (SC) are indicated as gray dots and pluses, respectively, in panel Q. Abbreviations: mBST - bed nucleus of stria terminalis, medial part; CnF - cuneiform nucleus; DA - dorsal hypothalamic area; d Hipp - dorsal hippocampus; DR - dorsal raphe; EPN - entopeduncular nucleus; FrA - frontal association cortex; IPAC - interstitial nucleus of the posterior limb of the anterior commissure; LC - locus ceruleus; LDTg - laterodorsal tegmental nucleus; LH - lateral hypothalamus; LHb - lateral habenula; LPO - lateral preoptic area; m-i Th - midline-intralaminar thalamic nuclei; PAG - periaqueductal gray; PB - parabrachial nucleus; PF - parafascicular nucleu; PPTg - pedunculopontine tegmental nucleus; Pr - nucleus prepositus; Rt - reticular formation; SC - subceruleus; Sol - nucleus of the tractus solitarius; VDB - vertical limb of the diagonal band; RMTg - medial tegmental nucleus; VP - ventral pallidum; VTA - ventral tegmental area; ZI - zona incerta.

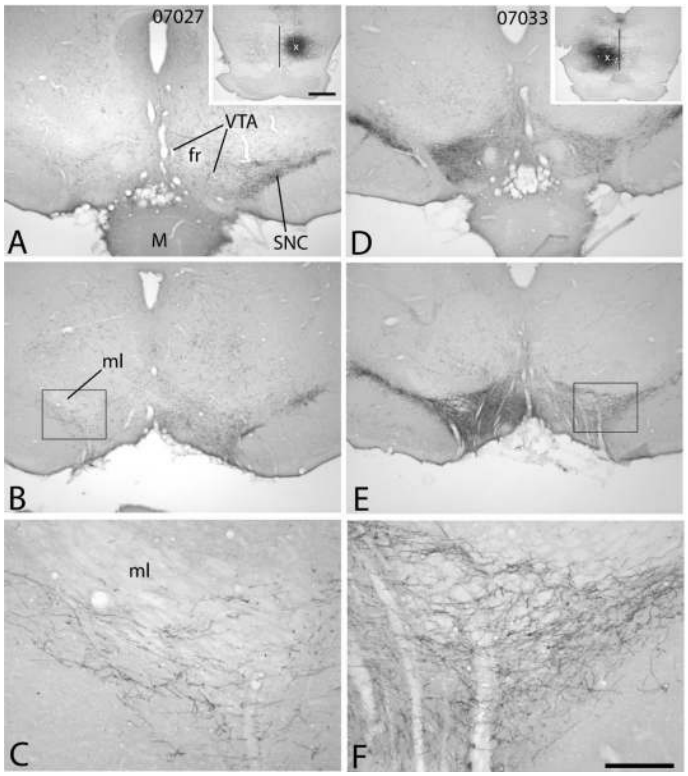

Figure 11.

Photomicrographs showing the projections from the rostromedial tegmental nucleus (RMTg) to the ventral tegmental area (VTA) - substantia nigra compacta (SNC) complex in two cases in which PHA-L was injected into the RMTg. Panels A–C illustrate case 07027, which is mapped in Figure 9 and has an injection site shown in Fig. 4 A–D. Panels A and B show more rostral and caudal levels of the VTA-SNC complex with ipsilateral anterograde labeling from the injection (shown in the inset in A) on the right. Contralateral labeling, within the box in B and enlarged in C, is less prominent. Panels D–E illustrate a similar injection (case 07033) that gives rise to denser ipsilateral (D and E, on the left) and contralateral anterograde labeling. The box in E is enlarged in F. Verticle lines and x in the insets approximate the midline and centers of the injections, respectively. The injection shown in panels A–C is centered slightly further from the midline and caudal relative to that shown in panels D–F. Additional abbreviation: fr - fasciculus retroflexus. Scale bars: 1mm in A–D, 200 μm in C and F (bar in F); 1 mm in insets (bar in inset A).

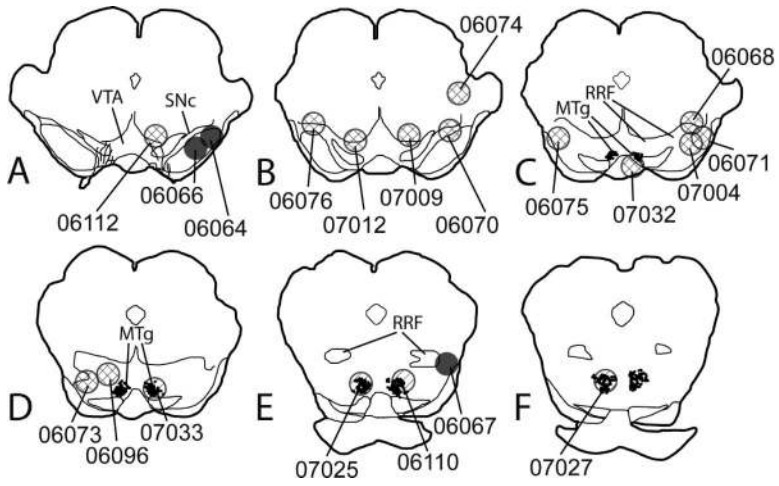

Figure 12.

Diagram depicting idealized sections though the mesencephalon and rostral pons with centers of PHA-L injection sites coded to reflect the amount of anterograde labeling that they gave rise to in the ventral tegmental area (VTA) - substantia nigra compacta (SNC) complex. Gray injections produced little or no labeling in the VTA-SNC complex. Cross-hatched sites produced sparse to moderate labeling, whereas simple-hatched sites produced robust VTA-SNC anterograde labeling. The medial tegmental nucleus (RMTg) is indicated by the clusters of black dots. The cases shown in this diagram are also included in Table 2, which considers additional cases and provides a more detailed treatment of VTA-SNC labeling.

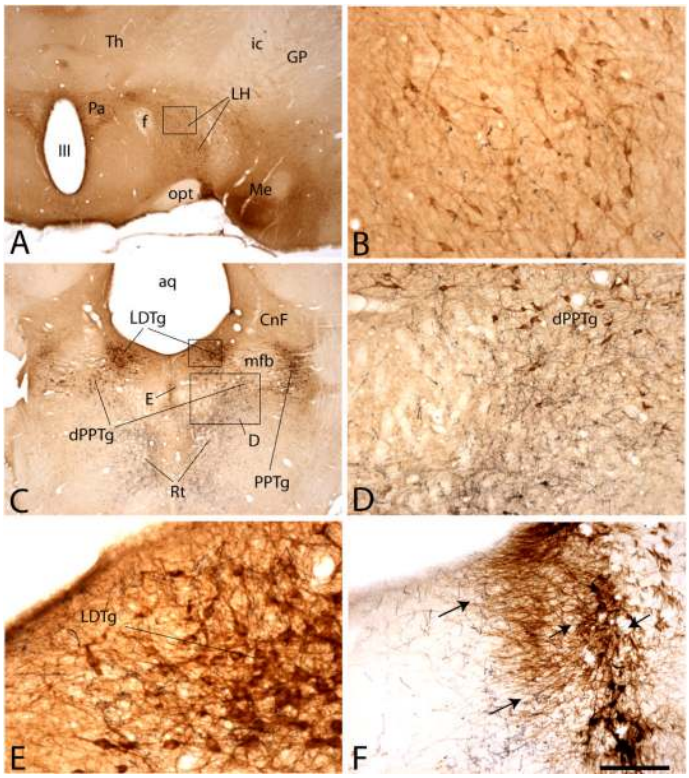

Figure 13.

Photomicrographs of sections processed for PHA-L (black), nitric oxide synthase (Nos) immunoreactivity (brown in A–E) or tyrosine hydroxylase (TH, in F) immunoreactivity showing anterograde labeling of axons in the lateral hypothalamus (A and B), mesopontine tegmentum (C–E) and locus ceruleus (F) in case 07027, in which PHA-L was injected into the medial tegmental nucleus (RMTg). The injection site for 07027 is illustrated in Figure 4 and the case is mapped in Figure 10. Note the moderate numbers of labeled projections to the lateral hypothalamus (LH) are (black fibers in B) in comparison to the robust labeled projection within in the mesopontine reticular formation (Rt). The mesopontine labeling substantially invades the laterodorsal tegmental nucleus (LDTg in E, an enlargement of Box E in panel C) and the dissipated part of the pedunculopontine tegmental nucleus (dPPTg in D, an enlargement of box D in panel C), which extends between the LDTg and PPTg and contains scattered Nos-ir neurons. Panel F shows the locus ceruleus, processed for TH-ir (brown) and PHA-L-ir (black fibers), from the same case. Robust axonal labeling can be seen in the region containing the distal parts of TH-ir dendrites (long arrows) and with in the cell dense part of the locus ceruleus (short arrows). Additional abbreviations: III - 3rd ventricle; aq - cerebral aqueduct; CnF - cuneiform nucleus; f - fornix; GP - globus pallidus; ic - internal capsule; Me - medial amygdala; mfb - medial forebrain bundle; opt - optic tract; Pa - paraventricular nucleus; Th - thalamus. Scale bars: 1 mm in A and C, μ200 m in B and D, 400 μm in E and F (bar in F).

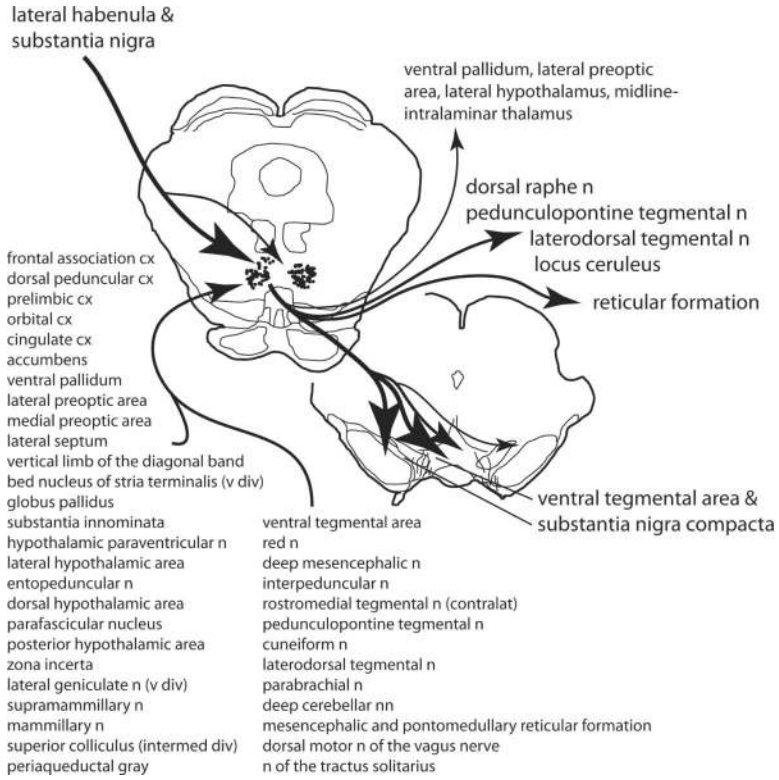

Figure 14.

Summary diagram illustrating the input-output relationships of the rostromedial tegmental nucleus (RMTg). Inputs are given on the left, outputs on the right. Line widths and arrowhead sizes represent approximations of the relative robustness of the pathways. Anatomical data suggest that the major RMTg throughput involves strong inputs to the RMTg from the lateral habenula, supplemented by projections from neurons scattered along the interface between the substantia nigra compacta and reticulata, and strong outputs to the ventral tegmental area/substantia nigra compacta complex. Numerous other forebrain and brainstem structures (listed on lower left in approximate rostrocaudal order) also project varyingly strongly to the RMTg, which has about equivalently strong outputs to the dorsal raphe, pedunculopontine tegmental nucleus, laterodorsal tegmental nucleus and locus ceruleus, which give rise to ascending neuromodulatory ("state-setting") pathways, and to the medial part of the mesencephalic and pontomedullary reticular formation, which gives rise to extensive, diffusely organized "level-setting" pathways to lower brainstem and spinal cord (see Discussion). Relatively meager outputs to the forebrain, by comparison, include the ventral pallidum, lateral preoptic area, lateral hypothalamus and midline-intralaminar thalamic groups. Abbreviations: contralat - contralateral, cx - cortex, div - division, intermed - intermediate, n - nucleus, nn - nuclei.

Table 1

Retrograde labeling following injections of Fluoro-Gold in the MTg and sites adjacent to it.

	MTg-centered injection sites			Control injection sites				
Structure	**08019**	**08023**	**08025**	**06160**	**06164**	**06166**	**08022**	**08031**
frontal association cortex	+++	+++	+++	++	+	++	++	++(v)
prelimbic cortex	+++	+++	+++	+	+	+	+++	++
dorsal peduncular cortex	+++	+++	+++	o	o	o	+++	++
anterior cingulate cortex	+++	+++	+++	++	+	++	+	+
accumbens	+	++	+	o	o	o	++	+
lateral septum	+	+	+	o	o	++	++	++
medial septum-diagonal band	++	+++	+++	o	o	o	++	++
ventral pallidum	++	++	+++	+	o	++	+++	++
lateral preoptic area	+++	+++	+++	+	o	+++	+++	o
medial preoptic area	++	+++	+++	+	o	+++	+++	o
bed nucleus of stria terminalis, ventral	+	+	+	+	+	+++	+++	o
bed nucleus of stria terminalis, medial	+	+	o	o	o	+	+++	o
median preoptic nucleus	+	++	+	o	o	+	+++	+
lateral hypothalamus	+++	+++	+++	+	+	+++	+++	++
sublenticular region	++	++	++	+	+	+++	+++	o
globus pallidus	+	+	+	+	o	+	+	o
hypothalamic paraventricular n	+	++	+	+	o	++	++	o
hyp. paraventricular n, posterior part	+	++	+	++	o	++	+++	o
entopeduncular nucleus	+	+	+	++	+	++	+	o
zona incerta	+++	+++	+++	++	++	++	++	+
lateral habenula	+++	+++	+++	+	++	++	+++	+
parafascicular n	++	++	++	++	o	+	+++	o
posterior hypothalamic area	++	+++	++	+++	+++	+++	+++	++
supramammillary n	+++	+++	+++	o	o	o	+++	++
mammillary body	+++	+++	++	o	o	o	+++	++
central gray (hypothalamus)	+++	+++	++	++	+	+	++	+
ventral lateral geniculate n	++	++	+	o	++	o	o	o
substantia nigra (compacta & reticulata)	++	++	++	+++	+++	+	++	o

	MTg-centered injection sites			Control injection sites				
Structure	**08019**	**08023**	**08025**	**06160**	**06164**	**06166**	**08022**	**08031**
ventral tegmental area	+	++	++	++	+	++	++	o
interpeduncular nucleus	+++	+++	++	o	o	o	+	n/a
medial tegmental nucleus	+(c)	++(c)	++(c)	o	o	o	+(b)	+
superior colliculus, deep, contralateral	+++	+++	+	+	++	o	+++(b)	o
periaqueductal gray	+++	+++	++	+++	++	++	+++	++
deep mesencephalic nucleus	++	++	++	+++	++	++	+++	++
dorsal raphe	+	+++	++	+	+	+++	+++	++
pedunculopontine tegmental nucleus	++	++	++	++(r)	+	++(r)	+	+
laterodorsal tegmental nucleus	++	+++	++	++	+	+	++	++
median raphe	++	++	+	+	+	+	++	+++
cuneiform n	++	++	+	++	o	+++	++	o
parabrachial n	+++	++	+	++	++	++	+++	o
principal trigeminal n	++	+	+	o	+	o	o	o
n prepositus	++	++	+++	o	o	o	++	+++
deep cerebellar n	+++(b)	+++(b)	++	++(i)	++(c)	++(c)	++(u)	o
pontomedullary reticular formation	++	++	+	++	++	++	++	+

Injection sites are illulstrated in Fig. 6. o = absent or trace retrograde labeling reflecting 0, 1 or 2 labeled cells/structure. + = 1 to 5 labeled neurons/section. ++ = 6–20 labeled neurons/section. +++ = more than 20 labeled neurons/section/structure. This list provides the main ipsilateral structures, listed in approximate rostocaudal sequence, labeled after injections in VMTg. Representative contralateral labeling is illustrated in Figure 9. Structures in addition to those in the list include for the control cases: 06160 - motor cortex ++, ventrolateral caudate-putamen +, posterior intralaminar thalamic n +++, deep layers of superior colliculus (i) +++; 06164 - motor cortex ++, deep layers of superior colliculus (i) ++; 06166 - dorsolateral division of the bed nucleus of stria terminalis +++, interstitial nucleus of the posterior limb of the anterior commissure ++, medial division of the central nucleus of the amygdala ++; 06167 - motor cortex ++; 08022 - dysgranular insular cortex ++, dorsolateral division of the bed nucleus of stria terminalis ++, interstitial nucleus of the posterior limb of the anterior commissure ++, thalamic paraventricular nucleus ++; 08031 - deep insular cortex +, medial habenula +++. Abbreviations: b - bilateral; c - contralateral mainly; i - ipsilateral; r - rostral; u - unilateral (interesting, because the injection was in the midline); v - ventral.

Table 2

Brainstem projections to the VTA-nigral complex

		Ipsilateral		Contralateral	
Case	**PHA-L Injection site**	**SNc**	**VTA**	**VTA**	**SNc**
05093	lSNR	0	0	0	0
06064	dl SNR & adjacent SNC	+	+	+	+
06066	vm SNR	++	+	+	0
06067	peripeduncular nucleus	0	0	0	0
06068	l RRF	++	+	+	+
06070	l SNC & adjacent SNR	++	+	+	+
06071	l RRF	++	+	+	+
06073	cl SNC	++	+	+	+
06074	deep mesencephalic nucleus	++	++	++	++
06075	c SNC & adjacent RRF	++	+	+	+
06076	l SNC, adjacent RRF	++	+	+	+
06096	RRF, mid m-l	+++	+++	++	+
06110	RRF, mid m-l; **MTg**	+++	+++	+++	+++
06112	RRF, mid m-l, large	+++	++	+	+
07004	l SNC & RRF	+++	++	++	+
07009	c RRF, mid m-l,	++	++	++	+
07012	RRF, mid m-l, small	++	++	+	+
07025	cmv RRF, large; **MTg**	+++	+++	++	++
07027	**MTg**, behind RRF	+++	+++	+++	+++
07032	l IPN, adjacent VTA & **r MTg**	++	+++	++	++
07033	**MTg**	+++	+++	+++	++
07046	VTA, center	++	Ø	+	+
07050	m lemniscus	0	0	0	0
07052	m lemniscus	+	+	+	+
07055	l IPN, adjacent VTA; **MTg**	++	++	++	++
07056	m lemniscus	+	+	+	+
07057	vl VTA & rl IPN	+++	Ø	+	+
07072	IPN	+	+	+	0

		Ipsilateral		Contralateral	
Case	**PHA-L Injection site**	**SNc**	**VTA**	**VTA**	**SNc**
07077	cm VTA	+	+	+	+
07078	dc RRF; **MTg**	++	++	++	++
08038	midbrain tegmentum beneath Fos-tail	+	+	+	+
08035	d paramedian raphe	++	++	+	0
08039	pontine tegmentum	+	+	+	+
08046	red nucleus	+	+	+	+
08047	IPN & **MTg**	++	+++	+++	+
08052	m VTA	++	Ø	+	+
08053	**r MTg**	++	+++	+++	+
08054	IPN & VTA	++	Ø	+	0

Substantial involvement of ventromedial tegmental nucleus (VMTg) indicated by **bold.** + = mean of <10 labeled fibers/section; +++ = mean of 11–50 labeled fibers/section; +++ = mean of >50 labeled fibers/section. Abbreviations: c - caudal; d - dorsal; IPN - interpeduncular nucleus; l - lateral; m - medial; RRF - retrorubral field; SNR & SNC - substantia nigra, pars reticulata & compacta; v - ventral; VTA -ventral tegmental area; Ø - obscured by injection site

Table 3

Representative archived anterograde labeling cases confirming projections to MTg.*

Case	Tracer / Injection site	Case	Tracer / Injection site
93158	BDA / VP	20015	PHA-L / BST
94020	BDA / VP	03153	PHA-L / LPH
94031	BDA / VP	03154	PHA-L / VDB
94052	BDA / VP	04265	PHA-L / PrL
97153	PHA-L / Acb	04266	PHA-L / PrL
97165	PHA-L / Acb	05020	PHA-L / VP
97172	PHA-L / Acb	06046	PHA-L / VP
99083	PHA-L / BST	06048	PHA-L / LPH

Abbreviations: Acb - accumbens; BDA - biotinylated dextan amine; BST - bed nucleus o stria terminalis; LPH - lateral preoptic-rostrolateral hypothalamic region; PHA-L - *Phaseolus vulgaris* - leucoagglutinin; PrL - prelimbic cortex; VDB - vertical limb of the diagonal band; VP - ventral pallidum.

*for methods and additional projections for cases 93158 - 94052, see Zahm et al. (1996); for cases 97153-20015, see Zahm et al. (1999) for cases 03153- 06048, see Geisler and Zahm (2005).